



IMPROVED DROUGHT EARLY WARNING AND FORECASTING TO STRENGTHEN
PREPAREDNESS AND ADAPTATION TO DROUGHTS IN AFRICA
DEWFORA

A 7th Framework Programme Collaborative Research Project

**Integration of drought forecasting tools for Africa into the Pan
African Map Viewer**

**WP6-D6.5
November 2013**



Coordinator: Deltares, The Netherlands
Project website: www.dewfora.net
FP7 Call: ENV-2010-1.3.3.1
Contract no.: 265454





Page intentionally left blank



DOCUMENT INFORMATION

Title	Integration of drought forecasting tools for Africa into the Pan African map server
Lead Author	JRC,
Contributors	ECMWF, ICPAC
Distribution	PP: Restricted to other programme participants (including the Commission Services)
Reference	WP6 – D6.5

DOCUMENT HISTORY

Date	Revision	Prepared by	Organisation	Approved by	Notes
09/04/2013		Gustavo Naumann	JRC		
21/10/2013		Gustavo Naumann	JRC		
21/10/2013		Luana Valentini	JRC		
21/10/2013		Diego Magni	JRC, Arcadia SIT		
23/10/2013		Emanuel Dutra	ECMWF		
11/11/2013		Emmah Mwangi	ICPAC		
15/11/2013		Reinder Brotsma	DELTARES		
20/11/2013		Paulo Barbosa, Gustavo Naumann	JRC		

ACKNOWLEDGEMENT

The research leading to these results has received funding from the European Union's Seventh Framework Programme (FP7/2007-2013) under grant agreement N°265454



Page intentionally left blank



SUMMARY

This report explores the integration of meteorological and hydrological seasonal forecasts into a single “pre-operational” drought monitoring and seasonal forecast system. An initial verification of the seasonal forecast clearly identified the regions and time scales that benefit from using precipitation forecasts from a dynamical model. These regions are mainly located in the tropics where climatic signals, such as El Niño-Southern Oscillation (ENSO), provide long-term predictability. On the other hand, our results also identified regions where the use of ERA-Interim for drought monitoring generates significant reductions of the forecasts skill

The use of specific drought indicators such as the Standardized Precipitation Index (SPI) instead of raw precipitation can give to local climate outlook forums, as the Greater Horn of Africa Climate Outlook Forum (GHACOF), reliable information about the intensity of the conditions expected in the forthcoming rainy season when available. Such information could then be used to support the decision process when issuing advisories for drought mitigation or adaptation actions within the region.

The Pan-African Map Viewer integrates drought monitoring and seasonal forecasting related information in an innovative approach for Africa, following a similar system developed for Europe through the European Drought Observatory (EDO). Such a monitoring and forecasting system provides multiple drought meteorological and hydrological products together with vulnerability and risk maps derived from socio-economic indicators. This information can be a useful input for existing and future drought early warning systems since it provides information on drought magnitude and extent, as well as understanding the potential drought impacts. Although the system is still under development it is already in a demonstrative pre-operational phase, with a variety of tools and drought related products that are accessible to end users and stakeholders interested in drought information in Africa.



Page intentionally left blank



TABLE OF CONTENTS

1.	INTRODUCTION.....	11
2.	SEASONAL FORECAST SYSTEMS	13
2.1	ECMWF SEASONAL FORECATS SYSTEM	13
2.2	DROUGHT INDICATOR (STANDARDIZED PRECIPITATION INDEX)	13
2.3	PCR-GLOBWB: PCRASTER GLOBAL WATER BALANCE MODEL	14
2.3.1	Delft-FEWS	14
2.3.2	PCR-GLOBWB	14
3.	SEASONAL FORECAST VERIFICATION	17
3.1	METHODS	17
3.2	RESULTS	20
4.	GREATER HORN OF AFRICA CLIMATE OUTLOOK FORUM (GHACOF).....	25
4.1	GHACOF BACKGROUND.....	25
4.2	DATA AND METHODS.....	26
4.2.1	Observations and model data.....	26
4.2.2	Quantitative assessment of the forecast skill	27
4.2.3	Qualitative assessment of skill.....	28
4.3	RESULTS AND DISCUSSION	29
4.3.1	System-4 verification against in situ observations.....	29
4.3.2	Use of system-4 in the consensus framework.....	33
5.	VISUALIZATION OF THE FORECAST INFORMATION INTO THE MAP VIEWER.....	38
5.1	SYSTEM ARCHITECTURE	38
5.2	WEB PORTAL AND FUNCTIONALITIES.....	38
5.2.1	DEWFORA Map Viewer	39
5.2.2	DEWFORA Time Series	44
5.2.3	DEWFORA Compare Layers.....	46
6.	CONCLUSIONS.....	50
7.	REFERENCES.....	52
8.	APPENDICE I – OVERVIEW AND DEVELOPMNET OF DEWFORA MAP VIEWER PRODUCTS	55



8.1	MONITORING PRODUCTS	56
8.2	SEASONAL FORECASTS	58
8.3	DROUGHT VULNERABILITY AND RISK.....	59
8.4	GEOGRAPHICAL BACKGROUND	60



LIST OF FIGURES

Figure 3-1 Regions used in the analysis adapted from Giorgi and Francisco (2000).....	18
Figure 3-2 Calendar month with maximum accumulated precipitation in the previous 3 (top panel) and 6 (bottom panel) months calculated as the mean over the regions using GPCC for the period 1979-2010.....	18
Figure 3-3 Seasonal forecasts evaluation resume for the SPI-3 over East Africa (top left - valid for May), West Africa (top right - valid for September) and South Africa (bottom left - valid for February). For each region, the forecast evaluation consist of 4 panels displaying a specific score as a function of lead time (horizontal axis- forecast initial date) for a specific verification date (in the title) for the GPCC+S4 forecasts (red), GPCC+CLM (black), ERAI+S4 (blue) and ERAI+CLM (grey). Top left: RMS error of the ensemble mean and ensemble spread about the ensemble-mean in dashed; top right: ROC; bottom left: Anomaly correlation; bottom right: ROC skill score (comparing GPCC+S4 with GPCC+CLM and ERAI+S4 with ERAI+CLM).	21
Figure 3-4 Seasonal forecasts evaluation summary for the SPI-6 (left) and SPI-12 (right) valid for August over East Africa.	22
Figure 3-5 - ROC scores of the SPI-3 (left), SPI-6 (centre) and SPI-12 (right) forecasts at different lead times (each line) given by GPCC monitoring the S4 precipitation forecasts. Regions with dashed pattern denote that the ROC score was given by GPCC+S4 forecasts is higher (with 95% confidence) than ERAI+S4 forecasts.	23
Figure 3-6 Last lead time where the ROC of the SPI seasonal forecasts given by GPCC+S4 are higher (at 95% confidence) than the forecasts given by ERAI+S4 for the (a) SPI-3, (b) SPI-6 and (c) SPI-12. The forecasts are verified for the calendar month represented in Figure 3-2.	24
Figure 3-7 First lead time where the ROC of the SPI seasonal forecasts given by GPCC+S4 are higher (at 95% confidence) than the forecasts given by GPCC+CLM for the (a) SPI-3, (b) SPI-6 and (c) SPI-12. The forecasts are verified for the calendar month represented in Figure 3-2. When GPCC+S4 ROC scores are never higher than GPCC+CLM the region is filled with grey.	24
Figure 4-1 Countries that participate in the Greater Horn of Africa Climate Outlook Forum (GHACOF; Outlined) and homogenous zones over East African Countries (Coloured Polygons) for which observations were available	27
Figure 4-2 Correlation coefficients between the precipitation anomalies derived from ECMWF SYS-4 forecasts and in situ measurements during the MAM season for the period 1982-2009. Black and white dots represent regions with statistically significant ($P < 0.05$) and insignificant ($P > 0.05$) values respectively.	30
Figure 4-3 As Figure 4-2 but for the OND season.	30
Figure 4-4 Continuous Ranked Probability Skill Score (CRPSS) for MAM (Top panel) and OND (Bottom panel). The box plots extend from the minimum (whiskers), percentiles 10, 30, 50 (white line), 70, 90 and maximum.	31
Figure 4-5 ROC scores for MAM (Left panel) and OND (Right panel). The box plots extend from the minimum (whiskers), percentiles 10, 30, 50 (white line), 70, 90 and maximum.....	32



Figure 4-6 Relative Operating Characteristics diagrams for MAM (Left panel) and OND (Right panel).	33
Figure 4-7 SYS-4 probabilistic precipitation forecast for 5 lead times (Top panel), SYS-4 3-month SPI forecast for 5 lead times (Middle panel), observed precipitation (Lower panel, left) and GHACOF consensus (Lower panel, right) all for OND 2000.	35
Figure 4-8 SYS-4 probabilistic precipitation forecast for 5 lead times (Top panel), SYS-4 3-month SPI forecast for 5 lead times (Middle panel), observed precipitation (Lower panel, left) and GHACOF consensus (Lower panel, right) all for OND 2006	36
Figure 4-9 SYS-4 probabilistic precipitation forecast for 5 lead times (Top panel), SYS-4 3-month SPI forecast for 5 lead times (Middle panel), observed precipitation (Lower panel, left) and GHACOF consensus (Lower panel, right) all for MAM 2009.	37
Figure 5-1 Main page of the Map Viewer. Layer list structure and Toolbar highlighted.....	39
Figure 5-2 Main page of the Map Viewer. Main tools and layer groups highlighted	40
Figure 5-3 Layer time selection and information visualization	41
Figure 5-4 Date selection for forecasting layers.....	42
Figure 5-5 Identify function example	43
Figure 5-6 Graph of GPCC Rainfall, GPCC SPI-3, ERAI Top Soil Moisture, and ERAI Temperature Anomaly from 2008 to 2013, drawn at the point with Lon 16.65 and Lat -1.16.....	45
Figure 5-7 Use of UGC advanced options: in the example the town of Gaborone is used to set the coordinates of the graph location, optional colours are set for GPCC Rainfall and ERAI Temperature Anomaly, and a subtitle is present. Moreover, the image shows the zoom.	46
Figure 5-8 Compare Layers: GPCC Total Precipitation and GPCC SPI-3 in September 2012 and September 2013 over Gabon. The legend is displayed only in one of the four maps.	47
Figure 5-9 Compare Layers: Example of sketching an affected area in map 1 and checking if it is detectable also in the other maps, where a different indicator (bottom-left map) or different dates (right maps) have been selected.	49
Figure 8-1 Monthly anomalies in SPI-3 (ERAI, GPCP, TRMM), SPEI (ERAI and GPCP) and Soil Moisture Anomalies (SMA) for July 2000, 2003, 2006 and 2009. Solid lines indicates the zero contour.	57
Figure 8-2. Drought Vulnerability Index at sub basin level as displayed in the map viewer with country boundaries and populated places.	60



LIST OF TABLES

Table 8-1 Characteristics of the products included in the Pan-African Map viewer 55



Page intentionally left blank



1. INTRODUCTION

Essential components of any drought early warning system are the forecasting systems provided by the meteorological and hydrological models. These models provide forecasts of the weather conditions that can lead to drought and can be expressed in the form of relevant drought indices. These specific indices, such as the Standardized Precipitation Index (SPI) or Soil Moisture Anomalies (SMA), can be used to issue early warnings by computing the probability that any relevant drought threshold could be exceeded.

The meteorological forecasts from the probabilistic systems developed at the European Centre for Medium-range Weather Forecasts (ECMWF) were produced at continental level. The hydrological component relies on the PCRaster Global Water Balance (PCR-GLOBWB) that is combined with the ECMWF forecast products. The methodology behind the model formulations and drought indicators calculation was assessed vastly during the lifetime of the project (See DEWFORA deliverables D4.1, D4.2, D4.3 D4.5, D4.7 and D6.3). However, even if the dynamical models have significantly improved in the past decade, their ability to forecast in the seasonal scale varies significantly, both temporally and spatially. This is due to different factors such as systematic errors that can be associated to the model internal physics, or to the response to the boundary forcings and initial conditions. Thus, a skill assessment of the forecasts is an essential verification step before using them in an “operational” drought early warning system.

The real value of the forecasts (rather than the skill) is determined by the performance of the indicators derived from the forecasts (Ogallo et al., 2008) and how they reach timely to the end-users. Qualitative aspects of climate forecast products, as well as their quantitative attributes, are important to help end users to interpret, apply, and ultimately judge them (Nicholls 1999). Since there are different relevant methods and indicators used to monitor and forecast drought, a common accepted approach to reach consistently the end-users is to make available different drought related information into a single information system. Such a system should be one of the main tools for the implementation of a drought monitoring, forecasting and early warning system and will assist stakeholders to make objective decisions for drought risk assessment and mitigation.

Within the framework of the DEWFORA project a Pan-African Map Viewer was developed. The system was adapted following the main features of the earlier developed European Drought Observatory (EDO). This web application gives access to drought data containing historical, real time monitoring and seasonal forecasts describing both meteorological and hydrological drought. In the future, it could also contain information on satellite born



vegetation conditions that can be analysed together with the above mentioned drought indicators in order to understand how droughts are affecting vegetation.

The main goal of this report was threefold. Firstly, an approach that applies the seasonal forecast to drought indicators such as the Standardized Precipitation Index and the Soil Moisture Anomalies was tested and validated. Secondly, the overall skill of the forecasts was assessed and their potential added value to regional climate forums as the Greater Horn of Africa Climate Outlook Forum was established. Thirdly, all the relevant information with potential to be used in early warning system was integrated into the DEWFORA Pan-Africa map system, in order to be tested pre-operationally during the lifetime of the project.

The report is organized as follows; Section 2 reviews the main features of the main forecast systems used in their two components: the meteorological seasonal forecasts produced by the ECMWF Ensemble Prediction System and the hydrological seasonal forecasts issued using the PCR-GLOBWB (PCRaster Global Water Balance) model. Sections 3 and 4 focuses on the meteorological forecast performance and discusses the added value of including it in the Great Horn of Africa Climate Outlook Forum. In Section 5 there is an introduction to the map viewer architecture and web portal functionalities. Finally, section 6 presents the main conclusions of the report.

Additionally, the reader can found an overview on the research aspects behind the information incorporated in the Map Viewer in Appendix I and explore the map server at <http://edo.jrc.ec.europa.eu/dewfora/php/index.php?id=4119>.



2. SEASONAL FORECAST SYSTEMS

2.1 ECMWF SEASONAL FORECASTS SYSTEM

Seasonal forecasting provides useful information about the "climate" that can be expected in the coming months. The seasonal forecast is not a weather forecast: weather can be considered as a snapshot of continually changing atmospheric conditions, whereas climate is better considered as the statistical summary of the weather events occurring in a given time period. The principal aim of seasonal forecasting is to predict the range of values which is most likely to occur during the next season. In some parts of the world, and in some circumstances, it may be possible to give a relatively narrow range within which weather values are expected to occur. Such a forecast can easily be understood and acted upon; some of the forecasts associated with strong El Niño events fall into this category. More typically, the probable ranges of the weather differ only slightly from year to year. Forecasts of these modest shifts might be useful for some but not all users.

ECMWF seasonal forecasts, based on an atmosphere-ocean coupled model, were used for the drought forecasting in this report, where we evaluate the recently implemented System 4, which became available in November 2011 (**S4**; Molteni et al., 2011). The horizontal resolution of the atmospheric model is TL255 (about 0.7° in the grid-point space, same as ERAI) with 91 vertical levels in the atmosphere. The ocean model has 42 vertical levels with a horizontal resolution of approximately 1°. The seasonal forecast generates 51 ensemble members in real-time, with 30 years (1981-2010, 15 ensemble members) of back integrations (hindcasts). The lead time is 7 months, including the month of issue. Molteni et al., (2011) present an overview of the model biases and forecast scores of S4. The DEWFORA report D4.2 and D4.4 provides an overview of the performance of S4 (compared with other 3 seasonal forecasts systems) in predicting precipitation on a pan-African scale.

2.2 DROUGHT INDICATOR (STANDARDIZED PRECIPITATION INDEX)

The meteorological drought forecasts are characterized in this report using the Standardized Precipitation Index (SPI, McKee et al 1993). In the calculation of the SPI for a specific k timescale, the total precipitation for a certain month m ($m=1, \dots, N$ where N is the number of months in the time series) is the sum of the precipitation for the period $[m-k+1$ to $m]$. For each calendar month (i.e. all Januaries, Februaries, etc.) the accumulated precipitation distribution is fitter to a probability distribution. The resultant cumulative probability distribution is then transformed into the standard normal distribution (mean zero with one standard deviation), resulting in the SPI.

The extension of the SPI from the monitoring period, i.e. past, to the seasonal forecasts range is performed by merging the seasonal forecasts of precipitation with the monitoring product and is a crucial step of the whole system. Firstly, both the forecasts and monitoring



products are interpolated to a common resolution. Secondly, some care needs to be taken to the biases in the seasonal forecasts. These biases can drift over time, i.e. change with lead time, and can jeopardize the prediction skill. Moreover, since the merging procedure involves two different precipitation datasets, care has to be taken to ensure that the two datasets have the same mean climate. This is achieved by performing a simple bias correction of monthly precipitation. DEWFORA report D4.3 and Dutra et al. (2013) provide a detailed description of these calculations and evaluation over selected basins in Africa.

2.3 PCR-GLOBWB: PCRASTER GLOBAL WATER BALANCE MODEL

Operational forecasts of hydrological parameters have been produced forcing the PCR-GLOBWB hydrological model in a FEWS client server setup with meteorological data provided by ECMWF. ECMWF has provided an ensemble of seasonal forecasts for the continent of Africa, based on an atmosphere-ocean coupled model 7 months ahead. The results are presented in the DEWFORA Map Server as described in Chapter 5.

2.3.1 Delft-FEWS

Delft-FEWS is an open shell for managing, data handling and guiding of forecasting processes (Werner et al., 2004). Delft-FEWS is used by a large number of operational forecasting centres and agencies around the world for various purposes such as forecasting hydrological storm surge, water quality, reservoirs, etc. For the setup of the current forecasting system the FEWS-GLOWASIS (client-server) was used. This is a global hydrological forecasting system configured within the forecasting environment Delft-FEWS. The system has been built as part of the EU-GLOWASIS project. The forecast system consists of a Master Controller, a Postgress database and 18 forecasting shells (i.e. computational cores) for efficient handling of ensemble forecasts and data processing. Several workflows have been setup for running the hydrological model PCR-GLOBWB for Africa using the precipitation, temperature and potential evaporation forecasts.

2.3.2 PCR-GLOBWB

PCR-GLOBWB is a grid-based model (coded in a dynamic modelling language that is part of the GIS PCRaster) of global terrestrial hydrology. It is essentially a leaky bucket type of model applied on a cell-by-cell basis. The model calculates for each grid cell ($0.5^\circ \times 0.5^\circ$) and for each time step (daily) the water storage in two vertically stacked soil layers (max. depth 0.3 and 1.2m) and in an underlying groundwater layer (of infinite capacity), as well as the water exchange between the layers and between the top layer and the atmosphere. The model also calculates canopy interception and snow storage. The input data includes precipitation, actual or potential evaporation, and snow and ice dynamics. The



meteorological forcing is supplied at a daily time step and assumed constant over a grid cell. Sub-grid variability is taken into account by considering separately tall and short vegetation, open water and different soil types. Canopy interception store is finite and subject to open water evaporation. The total specific runoff of a cell consists of saturation excess surface runoff, melt water that does not infiltrate, runoff from the second soil reservoir and groundwater runoff from the lowest reservoir. Groundwater reservoir characteristic response time is parameterized based on a world map of lithology. River discharge is calculated by accumulating and routing specific runoff along the drainage network taken from DDM30 and includes dynamic storage effects and evaporative losses from the GLWD2 inventory of lakes, wetlands and plain (van Beek and Bierkens, 2009). The model includes new schemes of sub-grid surface runoff, interflow and baseflow and incorporates explicit routing of surface water flow using the kinematic wave approximation. Also, it contains a routine for lateral transport of latent heat from which the water temperature and river ice thickness can be calculated (Sperna Weiland et al., 2010). Candogan Yossef et al. (2011) assessed the model skill to reproduce floods and droughts events. For this simulated discharge values were compared with observed monthly streamflow records for a selection of 20 large river basins that represent all continents and a wide range of climatic zones. They observed that the system has a markedly higher skill in forecasting floods compared to droughts, but the prospects for forecasting hydrological extremes are positive. Sperna Weiland, et al. (2010) studied the usefulness of data from General Circulation Models (GCMs) for hydrological studies, with focus on discharge variability and extremes. The hydrological model PCR-GLOBWB was used to simulate the discharge with a GCM ensemble mean as forcing data. The resulting discharges were compared with the Global Runoff Data Center (GRDC) discharge data. Even after bias-correction, the method performed less well in arid and mountainous areas.

The meteorological variables required to force PCR-GLOBWB are daily values of precipitation, evapotranspiration and temperature. Fifty one ensemble members of forecasted precipitation and temperature were provided by ECMWF. Based on extra-terrestrial radiation, minimum, maximum and mean temperature potential evapotranspiration has been estimated using Hargreaves model (Hargreaves and Allen, 2003). Hargreaves was preferred over Penman-Montheith following Trambauer et al., (2013, under review) as it has the advantage to be applied in data scarce regions, which is the case for several regions in Africa. From comparison by Droogers and Allen (2002) the Hargreaves reference evaporation estimates on a global scale suggest that Hargreaves formula should be considered in regions where accurate weather data cannot be expected.



The parameters that have been predicted are:

- Actual evapotranspiration;
- Soil moisture content top layer;
- Soil moisture content second layer;
- Surface water discharge;
- Water stress index.

Although absolute values have been calculated for each ensemble member these are not presented in this report. A classification of 'below normal', 'normal' or 'above normal' conditions was used based on the number of members that lie within predetermined thresholds (33.3 and 66.7 percentiles) based on historical runs forced by ERA Interim-GPCP dataset (Balsamo et al., 2010).



3. SEASONAL FORECAST VERIFICATION

3.1 METHODS

To show how different precipitation sources can lead to different drought estimations, in this study we have selected a mixture of observation and modelling datasets as input to the drought forecasting system. The first is an observational dataset that includes a product from the Global Precipitation Climatology Centre (GPCC, <http://gpcc.dwd.de>): the full reanalysis version 6 (Schneider et al., 2011) available since 1901 to 2010 globally on a 1°x1° regular grid. The second dataset is the ECMWF ERA-Interim reanalysis (ERA-Interim; Dee et al., 2011) that is available since 1979 to present expired month with an approximate resolution of 0.7°. Both GPCC and ERA-Interim are used for drought monitoring and merged with the ECMWF S4 seasonal forecasts or climatological forecasts (CLM - samples from past years of the observational dataset). Dutra et al (2013a) provides a detailed description of these calculations: i.e., merging of monitoring products with seasonal forecasts, the climatological forecasts and the SPI transformation. This analysis was initially developed on a basin scale, and this report presents the first results of the methodology applied on a global scale.

We generated seasonal re-forecasts of the SPI 3, 6 and 12 using four configurations:

- a) GPCC monitoring and S4 forecasts (GPCC+S4);
- b) GPCC monitoring and climatological forecasts (GPCC+CLM);
- c) ERA-Interim monitoring and S4 forecasts (ERA-Interim+S4);
- d) ERA-Interim monitoring and climatological forecasts (ERA-Interim+CLM);

All four configurations provide a 30 year hindcast period (1981 - 2010) with 15 ensemble members and includes forecasts issued every calendar month with 6 months lead time.

Considering the large dataset of hindcasts (4 configurations, 3 SPI time scales, 12 initial forecast dates for 30 years) the verification needed to be target to the specific drought application. Therefore, the evaluation of the seasonal forecasts focuses on large regions adapted from Giorgi and Francisco (2000; Figure 3-1). These regions were identified in terms of homogeneous precipitation regimes. They are wide enough to contain sufficient model grid points for the metrics calculated in the next sections to be statistically stable.

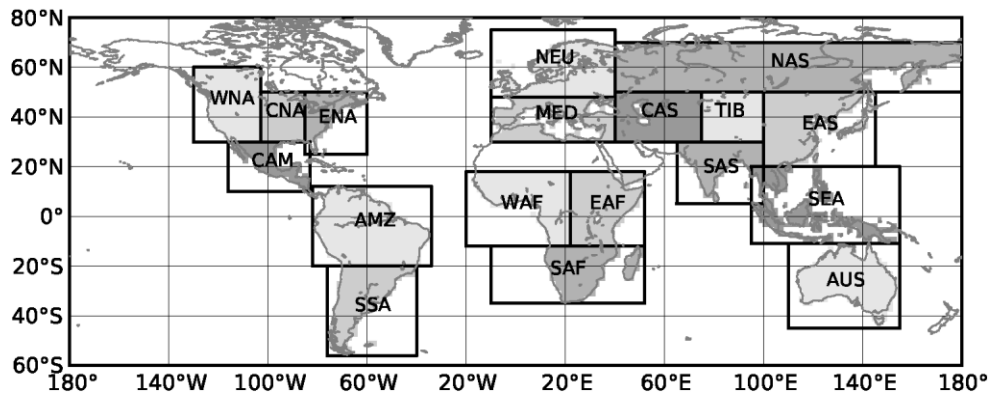


Figure 3-1 Regions used in the analysis adapted from Giorgi and Francisco (2000).

Moreover, the seasonal forecasts relevance and skills are dependent on the different seasons for each location. In a global analysis, the wide variety of precipitation regimes make it difficult to present the results synthetically for all the different initial forecast calendar months. Since this report is focused on drought events, we decided to verify the forecasts for target calendar months where precipitation anomalies are likely to have a higher impact. Using the mean annual cycle of GPCP precipitation in each region, we calculated the calendar month (in each region) with maximum accumulated precipitation in the previous 3 and 6 months, including the selected month (see Figure 3-2). The calendar month with 3 months maximum accumulated precipitation is used to verify the SPI-3 while the 6 months maximum accumulated precipitation the SPI-6 and SPI-12. Therefore, in the following results the spatial maps will display the scores for different initial forecast dates and verification dates, focusing on the lead times.

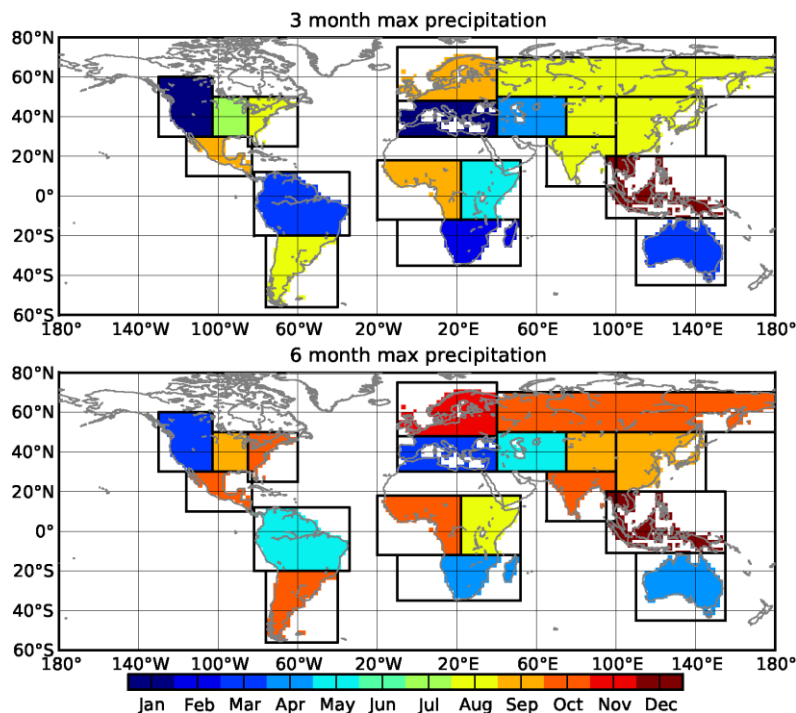


Figure 3-2 Calendar month with maximum accumulated precipitation in the previous 3 (top panel) and 6 (bottom panel) months calculated as the mean over the regions using GPCP for the period 1979-2010.

There is a large number of possible verification metrics that can be applied to probabilistic forecasts. In this report, we focus on the root mean square (RMS) error and anomaly correlation of the ensemble mean and the relative operating characteristics (ROC) of the SPI below -0.5.

The RMS error of the ensemble mean for a specific region, initial forecast calendar month and lead time is calculated as:

$$\text{RMS} = \frac{1}{n_t} \sum_{i=1}^{n_t} \left[\frac{1}{n_p} \sum_{k=1}^{n_p} (\overline{X(i,k)} - Y(i,k))^2 \right]^{0.5} \quad (3.1)$$

where n_t is the number of years (30), n_p is the number of points in the particular region $Y(i,k)$ is the GPCC based SPI for a specific year (i) and grid-point (k) and $X(i,k)$ the forecast ensemble mean. The RMS error confidence intervals are calculated for the temporal mean assuming a normal distribution. The time-mean of the RMS error of the ensemble mean should equal the time-mean ensemble spread about the ensemble-mean forecasts in a perfect forecast (Palmer et al., 2006). The time-mean ensemble spread about the ensemble-mean forecast is calculated as:

$$\text{RMS}(\text{spread}) = \frac{1}{n_t} \sum_{i=1}^{n_t} \left[\frac{1}{n_p} \sum_{k=1}^{n_p} \left\{ \frac{1}{n_e} \sum_{j=1}^{n_e} (\overline{X(j,i,k)} - Y(i,k))^2 \right\} \right]^{0.5} \quad (3.2)$$

where n_e is the number of ensemble members (15) and $X(j,i,k)$ is the forecast ensemble member (j) in year (i) and grid-point (k).

For the anomaly correlation, we first take calculate the grid-point Pearson correlation (r_k) in the form:

$$r_k = \frac{\sum_{i=1}^{n_t} (Y(i,k)' \overline{X(i,k)'})}{\left[\sum_{i=1}^{n_t} (Y(i,k)')^2 \right]^{0.5} \left[\sum_{i=1}^{n_t} (\overline{X(i,k)'})^2 \right]^{0.5}} \quad (3.3)$$

where the ' denotes the temporal anomaly (removing the temporal mean).

The grid-point r_k is then averaged over the particular region with the fisher and inverse-fisher transformation:

$$\text{Anom correlation} = \tanh \left(\frac{1}{n_p} \sum_{i=1}^{n_p} \text{arctanh}(r_k) \right) \quad (3.4)$$

The confidence intervals of the anomaly correlation are calculated by a 1000 bootstrap temporal re-sampling procedure (re-calculating equation (3.3) and (3.4) with random temporal sampling replacement).

ROC measures the skill of probabilistic categorical forecast, while the correlation (previous point) only considers the ensemble mean. The ROC diagram displays the false alarm rate



(FAR) as a function of hit rate (HR) for different thresholds (i.e. fraction of ensemble members detecting an event) identifying whether the forecast has the attribute to discriminate between an event or not. The area under the ROC curve is a summary statistic representing the skill of the forecast system. The area is standardized against the total area of the figure such that a perfect forecasts system has an area of 1 and a curve lying along the diagonal (no information) has an area of 0.5.

The results presented in the report refer to each region. This was achieved by using all the grid-points in a region when calculating the contingency tables for the FAR and HR estimates. The forecasts and verification fields were transformed into an event (or no event) based on underlying grid-point distributions. This spatial integration has the advantage of increasing the sample size used to build the contingency table while no spatial information is retained. To estimate the uncertainty of the ROC scores and the curves in the ROC diagram a 1000 bootstrap re-sampling procedure was applied. The contingency tables and the ROC scores were calculated 1000 times by temporal re-sampling: in each calculation the original forecast and verification grid-point time series are randomly replaced (allowing repetition) and a new set of scores is calculated. The re-sampling was performed only on the time-series, keeping all the grid-points, since the temporal sampling size (in our case only 30 values) is the largest source of uncertainty in the scores estimation. The 95% confidence intervals are estimated from the percentiles 2.5 and 97.5 of the 1000 ROC values (HIT and FAR).

3.2 RESULTS

An example of the RMS error, anomaly correlation, ROC and ROC skill score evolution with lead time for the SPI-3 forecasts in East Africa, West Africa and South Africa is displayed in Figure 3-3. In all regions there is a clear difference of the RMS error of the ensemble mean at lead times 0 and 1 between the forecasts using GPCC and ERAI for the monitoring, the latter with higher RMS errors. This is mainly due to the verification procedure that also uses GPCC. From lead time 2 onwards, the forecasts using S4 or CLM have the same RMS error independently of the monitoring datasets, since for those lead times only forecast precipitation is used. In both East and West Africa, the RMS error of ERAI+S4 decreases with forecast lead time, which might be contra intuitive. These results highlight the importance of the monitoring quality, which can affect significantly the SPI forecasts.

On the other hand, in South Africa the RMS error of ERAI+S4 increases with lead time which is in line with previous findings of the quality of ERAI over South Africa when compared with East or West Africa (see D4.3 report). The comparison of the RMS error of the ensemble mean with the ensemble spread (dashed lines in Figure 3-3) also suggests that the forecasts are under-dispersive. However, we do not consider the observations uncertainty (in this case the GPCC precipitation) that should be added to the ensemble spread when comparing with



the RMS error of the ensemble mean. The RMS evolution in East Africa for the SPI-6 and SPI-12 (see Figure 3-4) displays a similar behaviour to the SPI-3, with closer evolution of the S4 and CLM forecasts since for long SPI time scales both forecasts share more monitoring data.

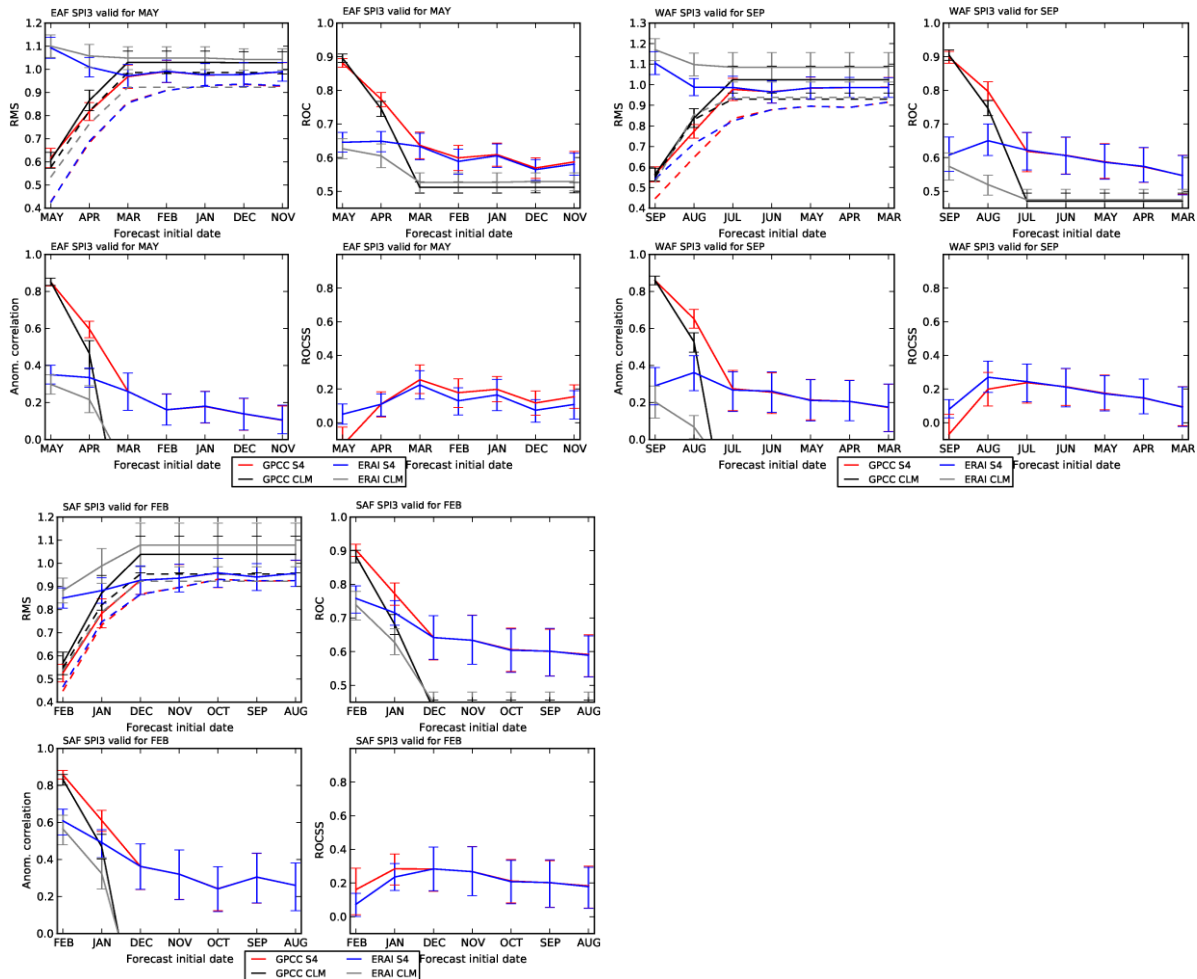


Figure 3-3 Seasonal forecasts evaluation resume for the SPI-3 over East Africa (top left - valid for May), West Africa (top right - valid for September) and South Africa (bottom left - valid for February). For each region, the forecast evaluation consist of 4 panels displaying a specific score as a function of lead time (horizontal axis- forecast initial date) for a specific verification date (in the title) for the GPCC+S4 forecasts (red), GPCC+CLM (black), ERAI+S4 (blue) and ERAI+CLM (grey). Top left: RMS error of the ensemble mean and ensemble spread about the ensemble-mean in dashed; top right: ROC; bottom left: Anomaly correlation; bottom right: ROC skill score (comparing GPCC+S4 with GPCC+CLM and ERAI+S4 with ERAI+CLM).

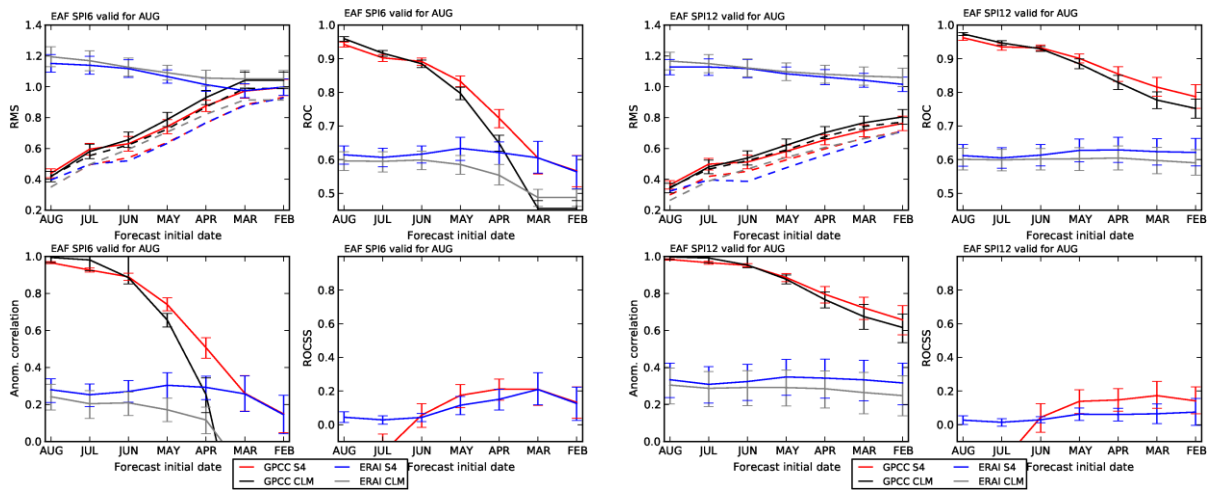


Figure 3-4 Seasonal forecasts evaluation summary for the SPI-6 (left) and SPI-12 (right) valid for August over East Africa.

The anomaly correlation of the SPI forecasts (in Figure 3-3 and Figure 3-4) using GPCC or ERAI monitoring also highlights the importance of the monitoring quality (as discussed before for the RMS errors). Similar results are found for the ROC scores that will be further compared in the following paragraphs.

A global overview of the GPCC+S4 ROC scores for the SPI-3, 6 and 12 for the different lead times is given in Figure 3-5. There is a clear difference in the skill decay with lead time that is lower for the SPI-12 than for the SPI-3. This is due to the fact that the longer time scales SPI use more GPCC monitoring data than the shorter time scales SPI. In Figure 3-5 the regions with a dashed pattern denote that the ROC score of the GPCC+S4 forecasts is significantly higher than the ROC scores of ERAI+S4 (with 95% confidence). To summarise this information, Figure 3-6 displays the last lead time (from 0 to 6 months) where the ROC of the SPI seasonal forecasts given by GPCC+S4 are higher (at 95% confidence) than the forecasts given by ERAI+S4 for the different SPI time scales. These results identify the regions where the use of ERAI for monitoring has a stronger detrimental effect on the skill of the seasonal forecasts. If ERAI would perform similarly to GPCC in terms of drought monitoring then the maps would show only short lead times. For all SPI time scales, in the tropical regions there is a clear signal of longer lead times with the GPCC+S4 with significantly higher ROC scores when compared with ERAI+S4 forecasts.

The ROC scores evolution with lead time in Figure 3-3 and Figure 3-4 showed that there is a reduced impact on skill for long lead times using different monitoring datasets, and for short lead times using the same monitoring dataset but different precipitation forecasts (CLM and S4). Figure 3-7 displays the first lead time where the ROC of the SPI seasonal forecasts given by GPCC+S4 are higher (at 95% confidence) than the forecasts given by GPCC+CLM. These lead times identify the added values of using seasonal forecasts of precipitation from a dynamical model for the SPI when compared to the climatological precipitation forecast.

For the SPI-3 in Northern Europe there is no benefit in using the S4 forecasts, while in all the remaining regions the S4 forecasts are beneficial. For the SPI-6 the use of S4 in Northern Europe and Central America also do not bring any added value to the climatological forecasts. For the SPI-12 this is also the case for the entire North America, North Eurasia, East Africa and Australia.

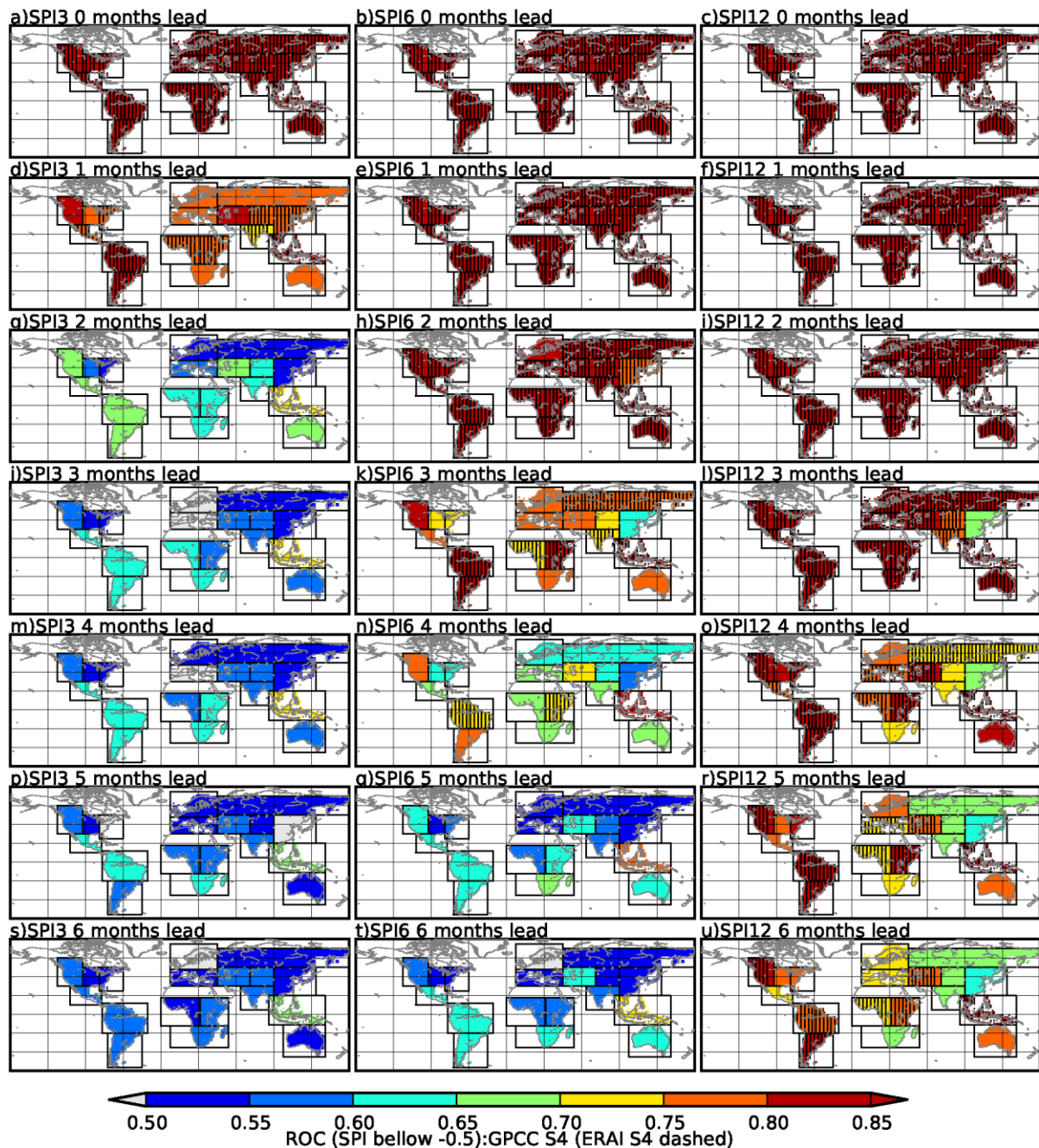


Figure 3-5 - ROC scores of the SPI-3 (left), SPI-6 (centre) and SPI-12 (right) forecasts at different lead times (each line) given by GPCCC monitoring the S4 precipitation forecasts. Regions with dashed pattern denote that the ROC score was given by GPCCC+S4 forecasts is higher (with 95% confidence) than ERAI+S4 forecasts.

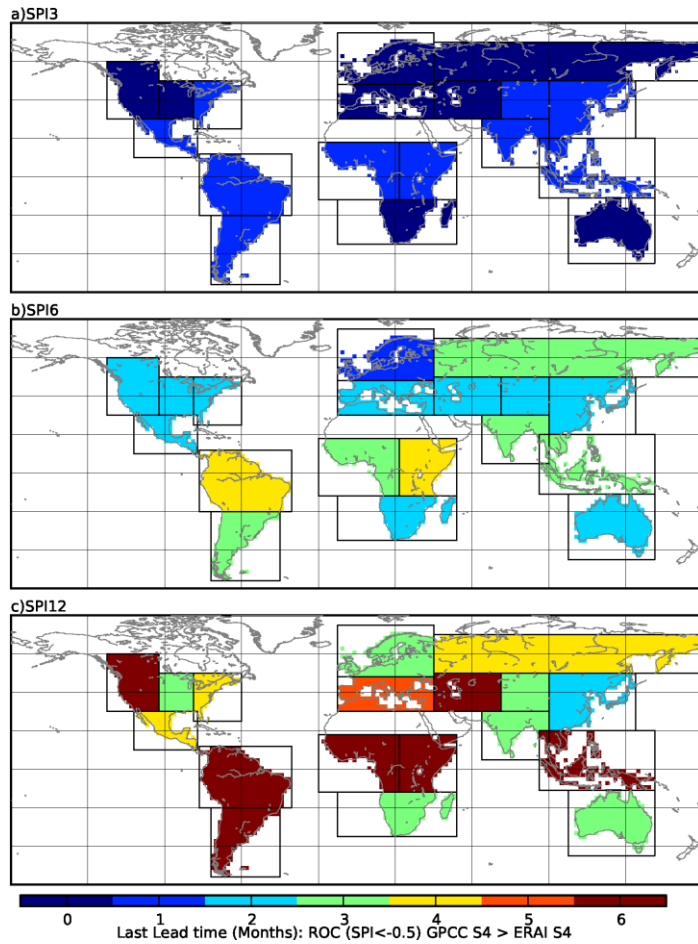


Figure 3-6 Last lead time where the ROC of the SPI seasonal forecasts given by GPCC+S4 are higher (at 95% confidence) than the forecasts given by ERAI+S4 for the (a) SPI-3, (b) SPI-6 and (c) SPI-12. The forecasts are verified for the calendar month represented in Figure 3-2.

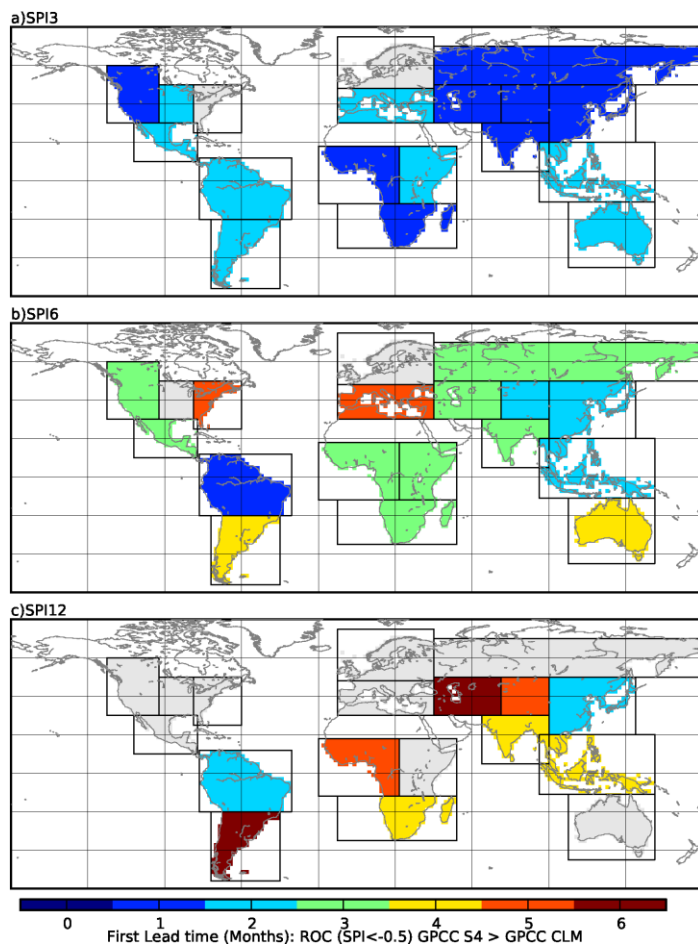


Figure 3-7 First lead time where the ROC of the SPI seasonal forecasts given by GPCC+S4 are higher (at 95% confidence) than the forecasts given by GPCC+CLM for the (a) SPI-3, (b) SPI-6 and (c) SPI-12. The forecasts are verified for the calendar month represented in Figure 3-2. When GPCC+S4 ROC scores are never higher than GPCC+CLM the region is filled with grey.

4. GREATER HORN OF AFRICA CLIMATE OUTLOOK FORUM (GHACOF)

4.1 GHACOF BACKGROUND

In a bid to ensure consistent access and interpretation of climate information, the World Meteorological Organisation (WMO) initiated Regional Climate Outlook Forums (RCOFs) in various parts of the world. To coordinate action over the Greater Horn of Africa region in which the East African countries are part of, the Greater Horn of Africa Climate Outlook Forums (GHACOFs, <http://icpac.sbis.co.kr>) are held three times a year before the relevant rainy periods (March-May, July-August, October-December). In preparation to each forum meteorologists from the National Meteorological and Hydrological Services (NMHSs) of Kenya, Uganda, Tanzania, Rwanda, Burundi, Ethiopia, Somali, Djibouti, Eritrea, Sudan and Southern Sudan (Figure 4-1) convene to issue a joint forecast for the incoming season. The forecast relies on a plethora of information. Firstly, there is the valuable forecaster's subjective knowledge and experience based on the past relationship between large scale sea surface temperature (SST) pattern and rainfall amount. Secondly, observed rainfall amount from the country's rain gauge networks is considered. Finally, data provided by dynamical forecast models from other international centres are taken into consideration. The outcome is consolidated into what is known as the *consensus forecast* for the Greater Horn of Africa (Ogallo et al., 2008). The main product is a map showing the probability for the rainfall of the incoming season to be in one of the terciles - above normal, near normal or below normal – of the rainfall distribution as observed by the local rain gauge network. The consensus forecast is then used by the national meteorological services to disseminate press releases with advisories of floods (droughts) expected in zones with forecasts above (below) normal conditions.

The consensus forecast is an excellent forum to share observed data and local knowledge to coordinate natural hazard related political actions in the region. It nevertheless mostly relies on precipitation monitoring and past experiences to construct drought scenarios for the upcoming season. Unexpected conditions, such as extreme events outside the climatology, are not taken into account in this approach and are likely to confound the forecaster's well established knowledge. Moreover, it does not contain information on the spatial extent and intensity of droughts as it is mostly based on station data. This study builds on the consensus forecast and explores the possible benefits of integrating the European Centre for Medium-Range Weather Forecasts (ECMWF) seasonal forecasting system product (SYS-4) into the forum. SYS-4 is issued at the beginning of each calendar month and provides an ensemble prediction of precipitation up to seven months ahead. If used in an automated system it could extend the consensus drought prediction lead time and provide monthly updates in between the official forecasters' consensus meetings.

4.2 DATA AND METHODS

4.2.1 Observations and model data

Although the East Africa region comprises five countries we could nevertheless source rain gauges data only from Kenya, Uganda and Tanzania. This dataset was used for the verification of SYS-4. A large part of East Africa experiences two distinct rainfall seasons. “Long rains” extend during March to May (MAM) while the season with “short rains” takes place from October to December (OND). These seasons are linked to the movement of the Inter Tropical Convergence Zone (ITCZ) northward and southward (Nicholson, 1996). As a part of the consensus effort the three countries have been subdivided into 34 homogeneous regions (see Figure 4-1 for the consensus forecast boundaries) in terms of the precipitation experienced. Monthly rainfall totals for each of these 34 homogeneous zones is available for the period 1961-2009 through dedicated surface synoptic observations (*synop*) located in positions to be representative for each sub region. This dataset provides both the climate information from which the consensus forecast anomalies are evaluated and the data against which the validation of the drought forecast itself was performed.

Past consensus outlooks and seasonal observation maps for the Greater Horn of Africa (GHA) region were sourced from the Intergovernmental Authority on Development (IGAD) Climate Prediction and Applications Centre (ICPAC). The observed precipitation was interpolated to areal means from synoptic stations and is given as a percentage of the long term mean; < 25% severely dry, 25-75% moderately dry, 75-125% normal, 125-175% moderately wet and >175% severely wet.

The model used in this study was the ECMWF seasonal forecast system-4 (SYS-4) which is a fully coupled system based on the Integrated Forecast System (IFS) cycle 36r4 atmospheric model version with TL255 corresponding to roughly 80km spatial resolution and the Nucleus for European Modelling of the Ocean (NEMO) ocean model, which has a horizontal resolution of approximately 1 degree, and 42 levels in the vertical, 18 of which are in the upper 200m. At the first of each month the system provides an ensemble of 51 simulations through initial condition perturbations coming from a combination of atmospheric singular vectors and an ensemble of ocean analysis. An extensive hindcast set of 30 years is also available for model calibration and verification. The set of hindcast are initialised using ERA Interim reanalysis for the period 1981–2010 and have 15 ensemble members. Details of SYS-4 can be found in Molteni et al. (2011). Performances of the system to drive drought monitoring and forecasting in several African basins can be found in Dutra et al. (2013a).

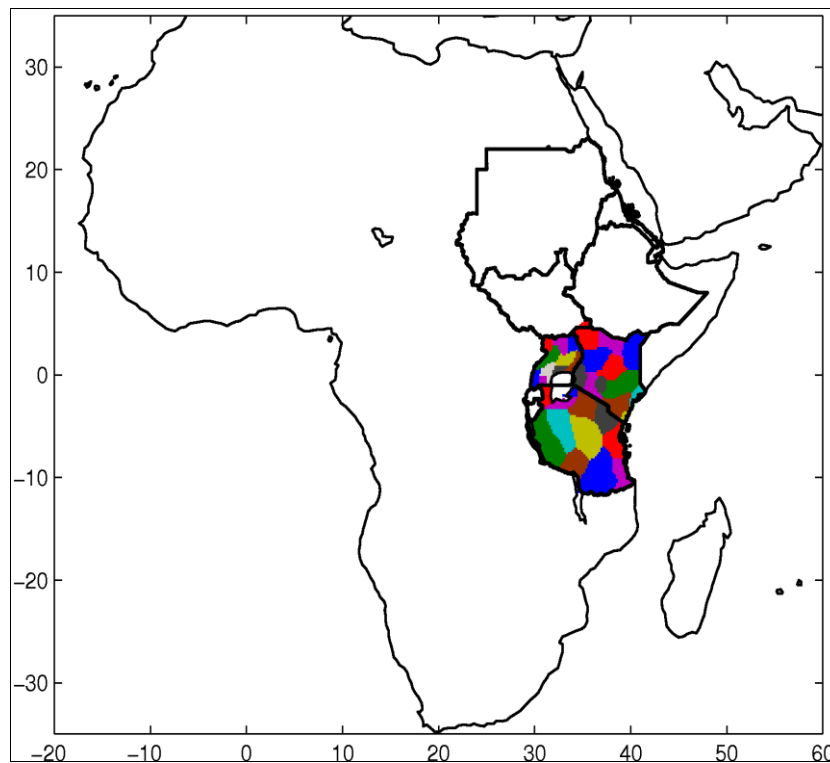


Figure 4-1 Countries that participate in the Greater Horn of Africa Climate Outlook Forum (GHACOF; Outlined) and homogenous zones over East African Countries (Coloured Polygons) for which observations were available

4.2.2 Quantitative assessment of the forecast skill

The skill of SYS-4 precipitation forecasts was evaluated using the standard skill scores methods based on the analysis of the correlation coefficient of the model and observations anomalies (ACC; Miyakoda et al., 1972) and the Continuous Ranked Probability Skill Score (CRPSS; Hersbach, 2000). The ACC provides information on the forecast skills of the ensemble mean (Hollingsworth et al., 1980 & Simmons, 1986) while the skill of the range of possibilities or uncertainty about that forecast value, that is, that of the ensemble members is provided by the CRPS. The skill score that corresponds to the CRPS is the CRPSS. $CRPSS = 1 - CRPS / CRPS_{ref}$. The most commonly used reference forecasts are persistence and climatology. If $CRPSS \leq 0$, no skill compared with reference forecast and if $CRPSS > 0$, some skill compared with reference forecast. The observation dataset, as a random sample of all years, was used to produce a climatological forecast with the same ensemble size as system 4. Another standard skill score employed is the area under the Relative Operating Characteristics (ROC) which is particularly effective if an estimate of false alarm occurrence is important. In probabilistic forecasting system, there are various thresholds for each forecast category. For each of the thresholds, the correspondence between the forecasts (a sequence of dry or non-dry) and observations (a sequence of events or non-events) is examined. The result is a two-component vector of the proportion of events for which a forecast was correctly issued ('hit rate') and the proportion of non-events for which a forecast



was incorrectly issued ('false-alarm rate'). The hit rate and false-alarm rate give the ROC curve. Details on ROC can be found in Mason and Graham (2002).

The SYS-4 precipitation skill over East-Africa was assessed employing the hindcast dataset for the period in which in situ measurements were available. Forecast interpolation at station location was done using the grid nearest-neighbour being the region homogeneous in terms of precipitation. Analogous analyses were performed using the average of 4 nearest points, and mean precipitation over the region (using the outlines in Figure 4-1) providing very similar results (not shown).

4.2.3 Qualitative assessment of skill

Much more challenging is instead the choice on how to quantify the added skill of using SYS-4 in the consensus framework. Both, the observed and the outlook maps were manually "smoothed". Since the original data-set to reconstruct them is not available, a quantitative assessment of the consensus maps is virtually impossible. Therefore, proxies of the consensus forecast maps were generated from SYS-4 forecasts for a subjective assessment on the basis of the added information they can provide in a hypothetical forecasters gathering. The exercise was repeated for the period 2000 to 2010 and for both seasons, March-April-May (MAM) and October-November-December (OND).

From the raw SYS-4 precipitation outputs dry and wet conditions were defined as the probability (or number of ensemble members) below the percentile 30 and above the percentile 70 of SYS-4's climatology for a particular season, respectively, and for the various lead times. To condense this information in a single map for each lead time, classes were defined as follows; moderately dry if 40% of the members predicted dry conditions and the dry cases were more than wet cases, severely dry if 60% of the members predicted dry conditions and extremely dry if 80% of the members predicted dry conditions. The same classification was applied for wet conditions and the rest was classified as normal (or uncertainty).

In addition to raw precipitation forecasts, maps of SPI were calculated from SYS-4 precipitation. SPI is the index recommended by WMO for Meteorological drought monitoring (Press report December 2009, WMO No. 872). Its calculation is based on long-term precipitation record which is fitted to a cumulative probability distribution and then transformed into a standard normal distribution with mean zero for each month (Edwards and McKee, 1997). Since the SPI is normalized, wetter and drier climates can be represented in the same way where positive (negative) SPI values indicate wet (dry) conditions respectively. SPI can be calculated for any desired duration, typically ranging from 1 to 48 month to reflect the impact of drought on the availability of the different water resources. Recently there has been increased focus on the use of Standardized Precipitation Index, in drought forecasting.



For example, Dutra et al. (2013a) proposed a methodology to forecast 3-month SPI for the prediction of meteorological drought over four basins in Africa: the Blue Nile, Limpopo, Upper Niger, and Upper Zambezi based on the SYS-4 forecasts of precipitation.

4.3 RESULTS AND DISCUSSION

4.3.1 System-4 verification against in situ observations

March, April, May (MAM) and October, November, December (OND) anomaly correlation coefficients (Figure 4-2 and Figure 4-3) and CRPSSs (Figure 4-4) are shown as a function of lead times. As expected the prediction skill declines with increasing lead time. The skill is higher in the OND than in MAM. Notable is that for both methods, there is higher skill in lead time of 2 than lead time of 1 month in the OND season. This is because of a spurious SYS-4's negative drift in SSTs over the NINO 3.4 region which highly impacts precipitation over East Africa. The fastest drift of SSTs occurs during the boreal summer months. A bias in the near-equatorial winds in the west and central Pacific is the dominant factor in driving an SST bias in the coupled model, whereby SSTs in the eastern equatorial Pacific drift to cold conditions (Molteni et al., 2011).

The skill of the categorical forecasts from ROC scores decline with increased lead time and there is higher skill for OND than MAM, as in the previous results (Figure 4-5 and Figure 4-6). Over 50% of the stations have considerable skill for OND season for all lead times; this is the case from January for the MAM forecast (Figure 4-5). SYS-4 has higher skill for the not dry (Normal and wet) category in MAM for all lead times (Figure 4-6). Since SYS-4 has a cold pool over Equatorial Pacific then the seasonal forecasts always have a higher skill for La Nina conditions, which are associated with dry conditions over East Africa. Thus the higher skill for not wet (Normal and dry) category in the OND season (Figure 4-6).

The high predictability in the horn of Africa is well documented and is due to the teleconnection between the Indian Ocean Dipole and the ENSO. Generally, the prediction skill of SYS-4 is better in the OND season than the MAM season (Dutra et al., 2013b) due to the documented strong relationship between the OND season rains and SST and ENSO (Mutai et al., 1998; Nicholson et al., 1990; Ogallo et al., 1988). While the MAM season rains have been associated with complex interactions between many regional and large-scale mechanisms which generally induce large heterogeneities in the spatial rainfall distribution (Beltrando, 1990; Ogallo, 1982) and virtually negligible correlations with ENSO (Ogallo et al., 1988).

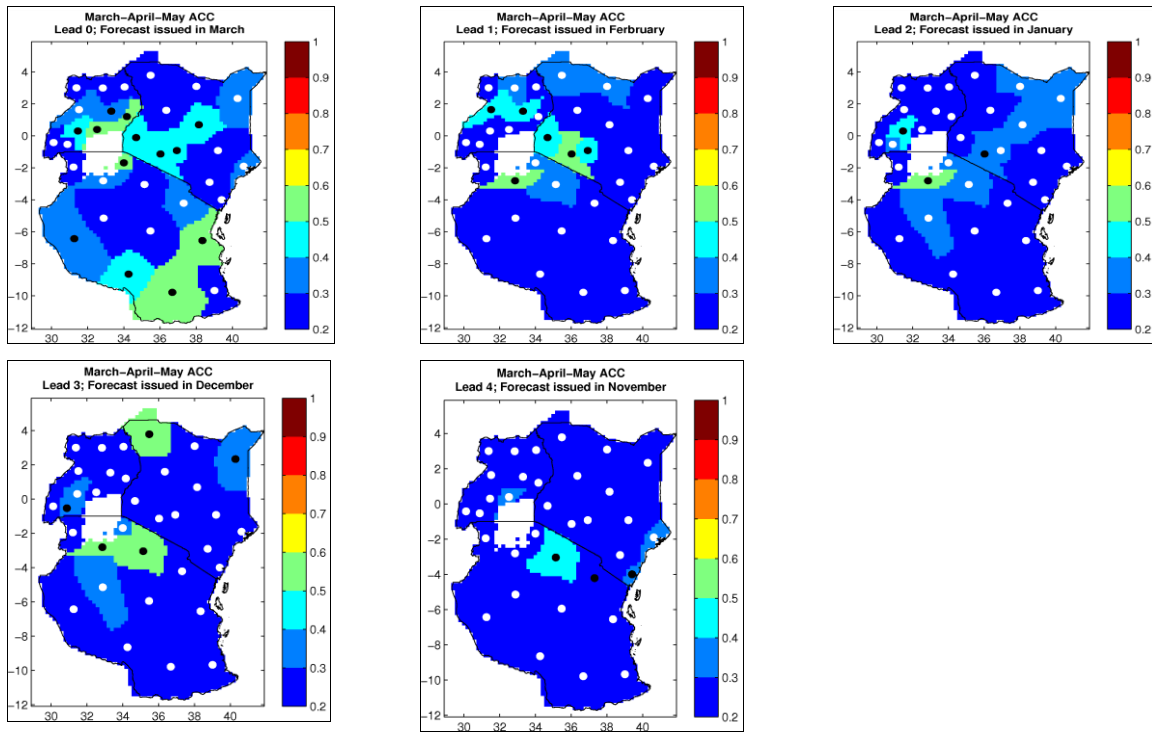


Figure 4-2 Correlation coefficients between the precipitation anomalies derived from ECMWF SYS-4 forecasts and in situ measurements during the MAM season for the period 1982-2009. Black and white dots represent regions with statistically significant ($P < 0.05$) and insignificant ($P > 0.05$) values respectively.

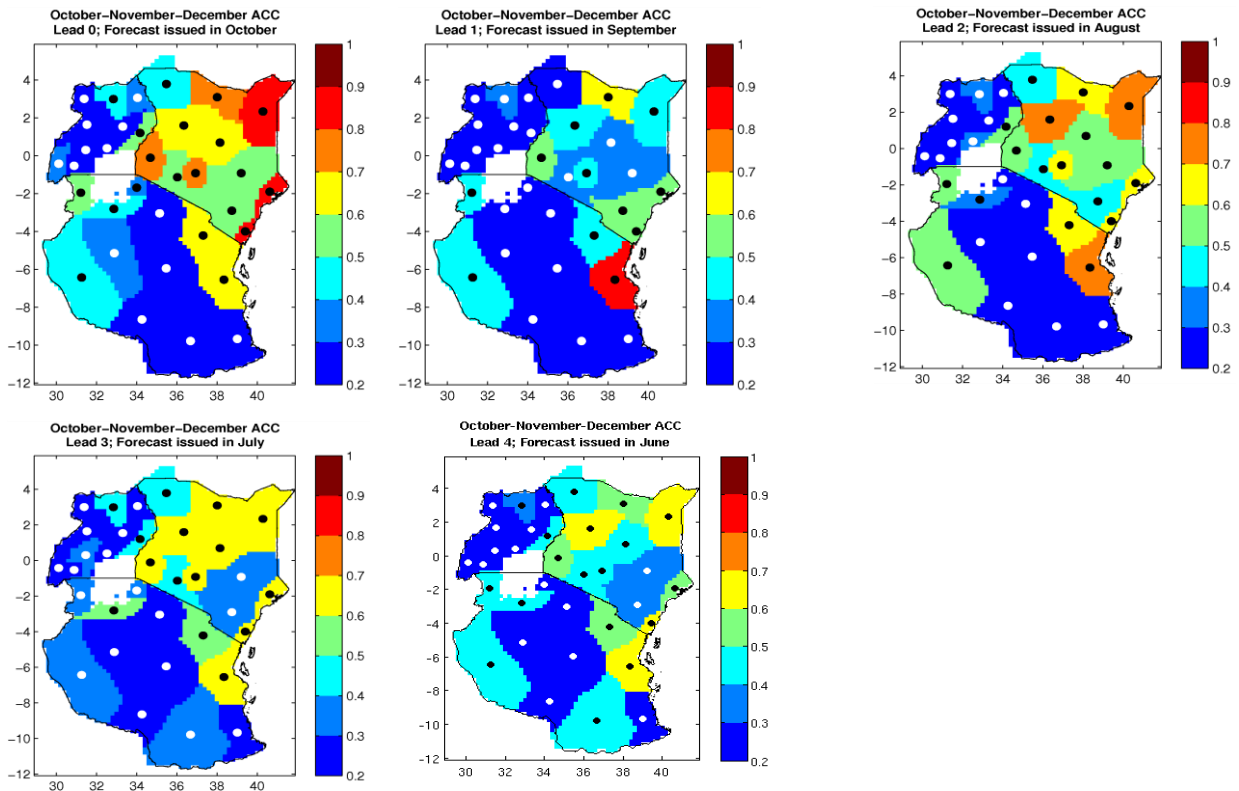


Figure 4-3 As Figure 4-2 but for the OND season.

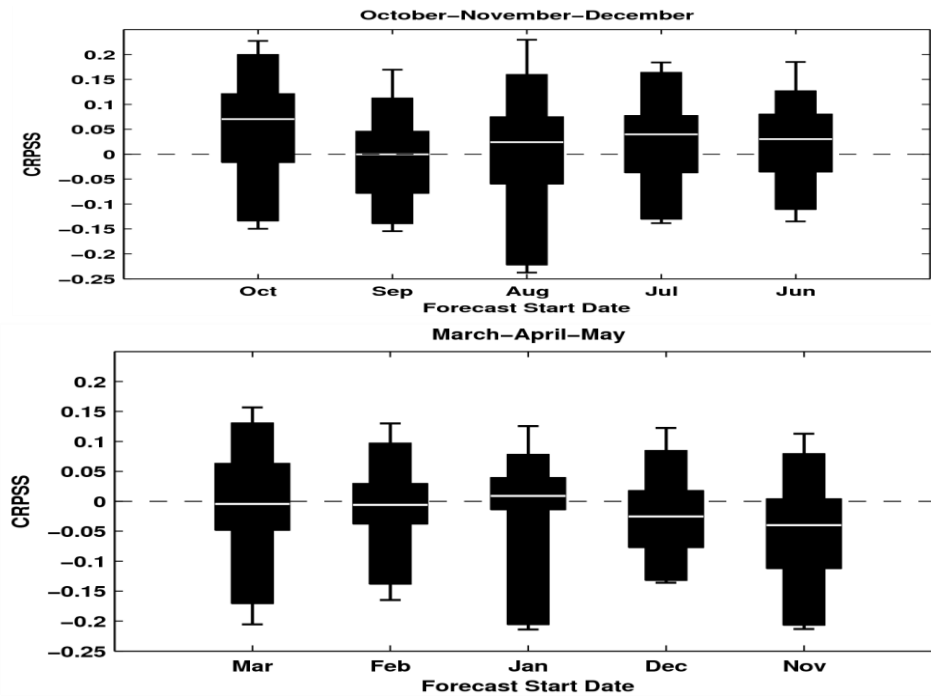


Figure 4-4 Continuous Ranked Probability Skill Score (CRPSS) for MAM (Top panel) and OND (Bottom panel). The box plots extend from the minimum (whiskers), percentiles 10, 30, 50 (white line), 70, 90 and maximum.

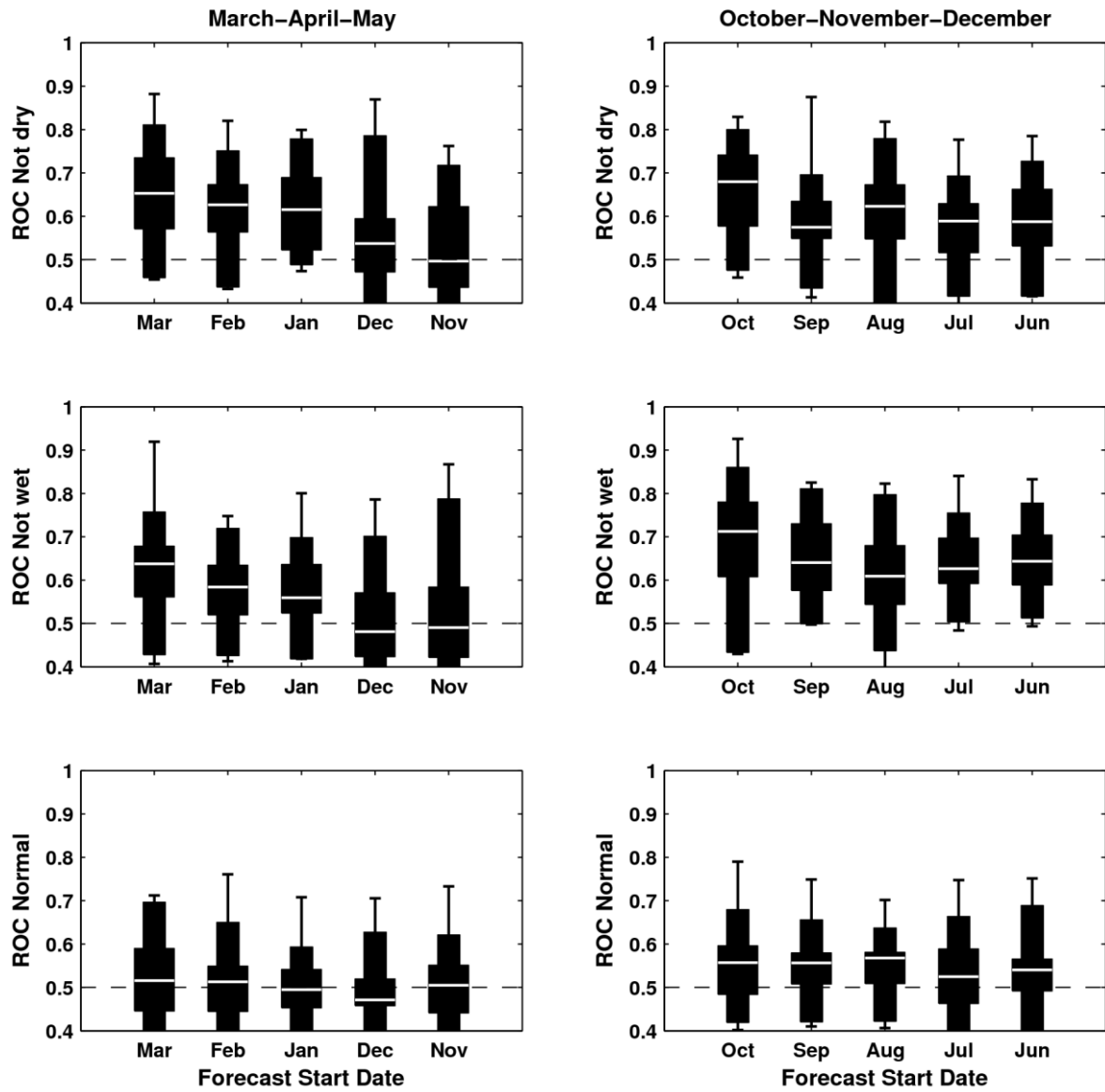


Figure 4-5 ROC scores for MAM (Left panel) and OND (Right panel). The box plots extend from the minimum (whiskers), percentiles 10, 30, 50 (white line), 70, 90 and maximum.

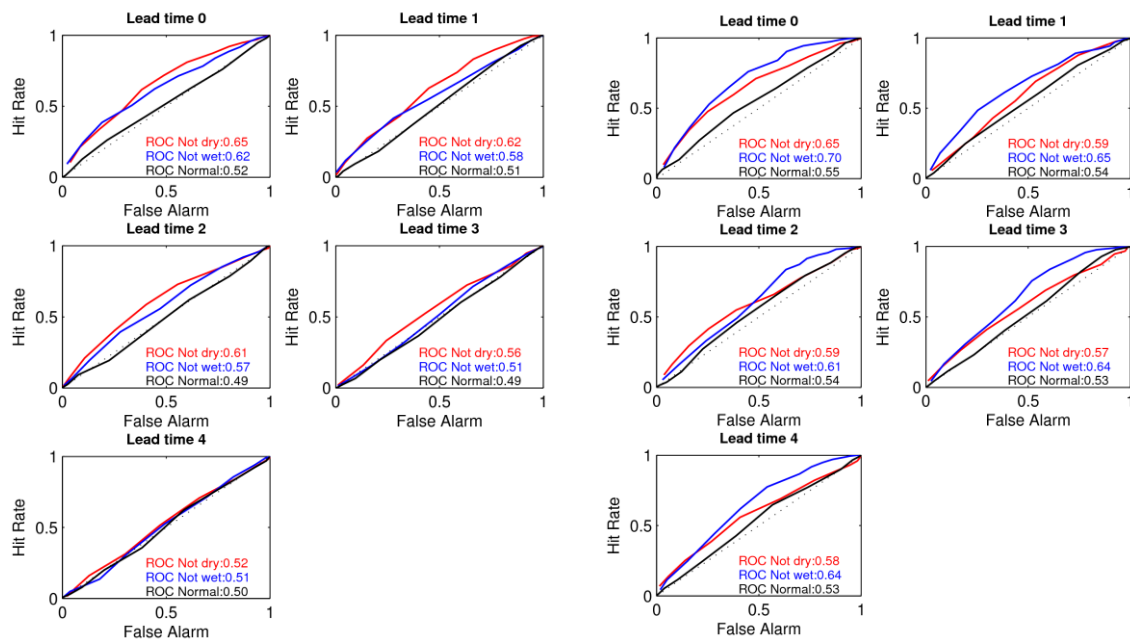


Figure 4-6 Relative Operating Characteristics diagrams for MAM (Left panel) and OND (Right panel).

4.3.2 Use of system-4 in the consensus framework

For the subjective nature of the ROC consensus forecasts a purely qualitative assessment of its skill was not possible. We therefore resorted to perform a qualitative analysis based on subjective examinations of 11 years of forecast. These analyses were performed independently by the 5 authors with the aim of judging the advantage SYS-4 would bring as an added product to the consensus framework.

Three cases were selected and discussed in details to showcase the value SYS-4 could have added to the consensus outlook if it had been provided as precipitation probabilistic forecast and as SPI forecast. The three cases selected were seasons with: below normal, normal and above normal precipitation.

In OND 2000, the observed precipitation was normal over most parts of the Greater Horn of Africa, except for some extremely wet patches over Ethiopia, Sudan and Tanzania (Figure 4-7). A significant area over North-eastern Kenya had moderately dry condition. SYS-4 precipitation forecast had a consistent signal for dry conditions over most of the region until August. September and October forecasts shift to normal conditions over the Eastern part and wet condition on the Northern and Western parts. Notable is that the two forecasts maintain a dry signal over Northern Kenya and the Tanzania and Kenyan coast. When the same analysis was repeated with the SPI, a similar forecast evolution to the precipitation is observed but spatially smoother. The consensus outlook predicted climatological conditions for the Northern part; wet conditions for the upper coastline and a small section of the Western part; and normal conditions for the rest of the region. If SYS-4 September and October forecasts would have been incorporated in the consensus forecast, then the outlook



could have been adjusted for the Kenya coast, Ethiopia and Sudan. That way the outlook would have been closer to the observations.

OND 2006 was a moderately wet season, from the observations most of the region experienced moderately wet conditions and much of the coastal area experienced severely wet conditions (Figure 4-8). The SYS-4 forecast had a wet signal far off in the ocean during June and August. The propagation inland happened in October. The same is seen in the SPIs however, the September forecast has a signal of moderately wet conditions inland. The consensus outlook forecasted normal conditions on most of the eastern part. If the consensus would have been updated in October using SYS-4 forecast, then the wet conditions observed on the Eastern part could have been captured.

MAM 2009 was a moderately dry season for the Eastern equatorial part of the region. Most of the Northern parts experienced severely dry condition and normal conditions were experienced on the western part (Figure 4-9). SYS-4 consistently captured the dry signal but it only propagated inland in January and March for both precipitation and SPI. The consensus outlook predicted dry conditions on over the Eastern and a section of the Northern part, the Western part had an above normal forecast. Combining the outlook and SYS-4's March forecast would have helped adjust the wet forecast over Ethiopia and Sudan to dry.

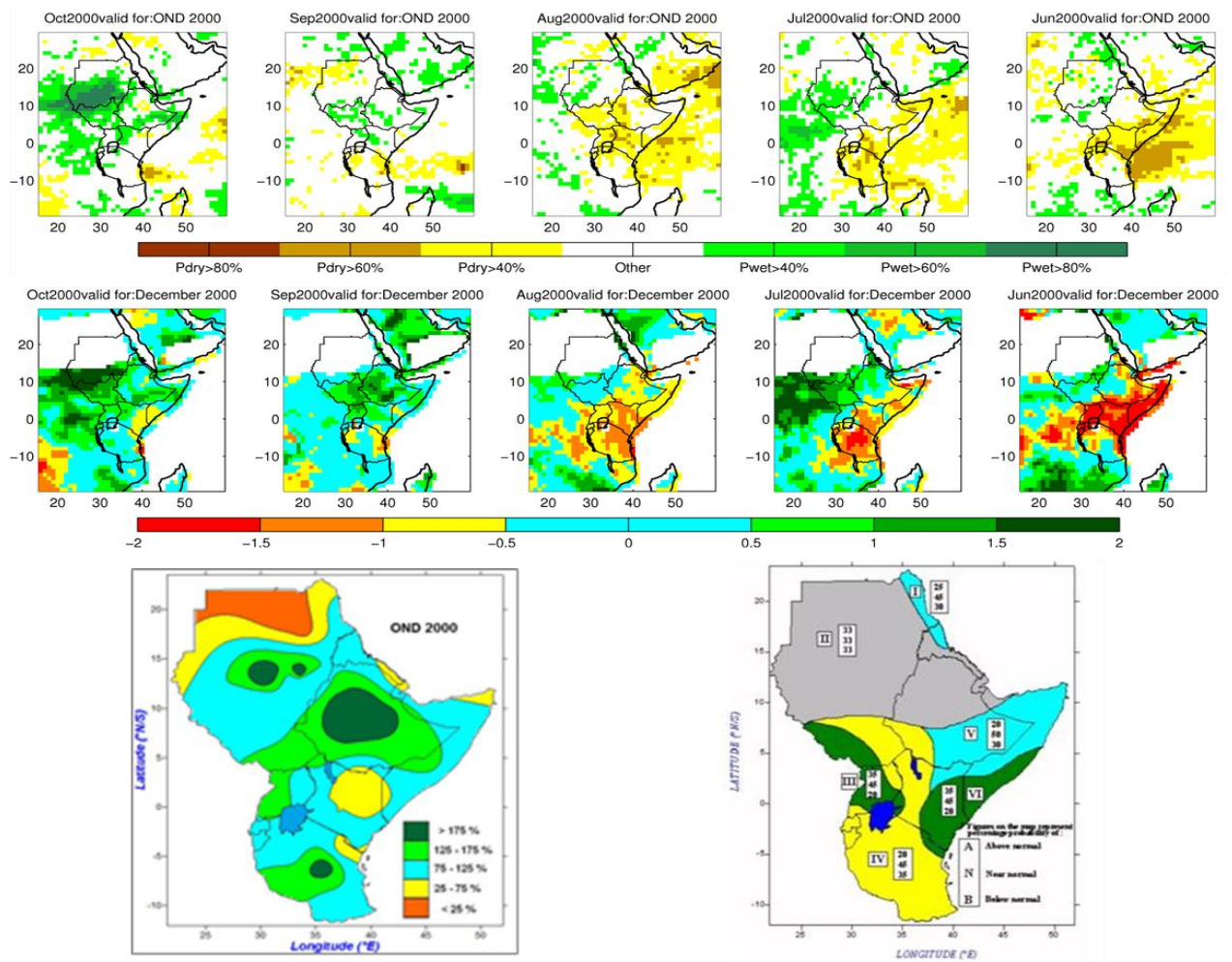


Figure 4-7 SYS-4 probabilistic precipitation forecast for 5 lead times (Top panel), SYS-4 3-month SPI forecast for 5 lead times (Middle panel), observed precipitation (Lower panel, left) and GHACOF consensus (Lower panel, right) all for OND 2000.

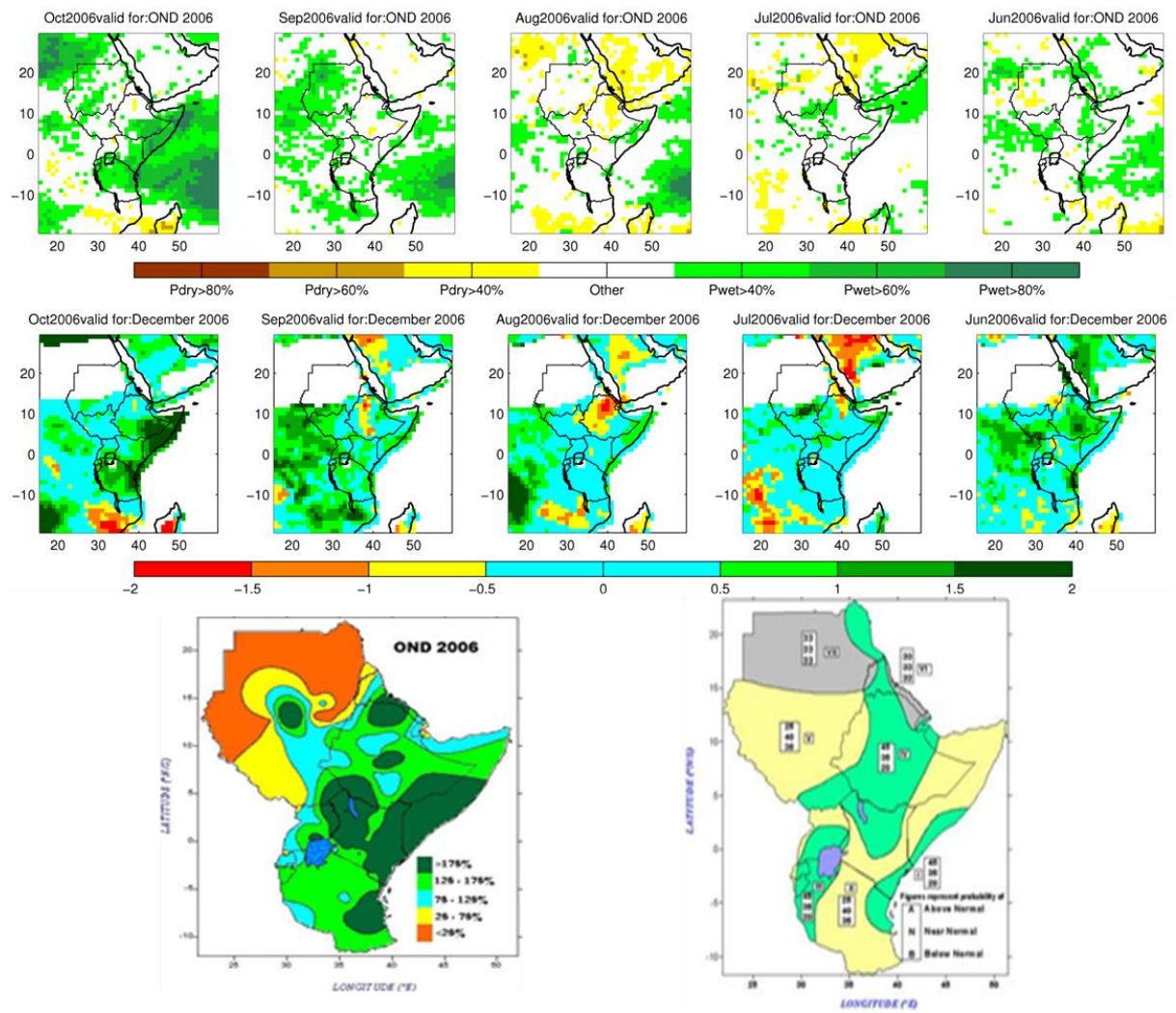


Figure 4-8 SYS-4 probabilistic precipitation forecast for 5 lead times (Top panel), SYS-4 3-month SPI forecast for 5 lead times (Middle panel), observed precipitation (Lower panel, left) and GHACOF consensus (Lower panel, right) all for OND 2006

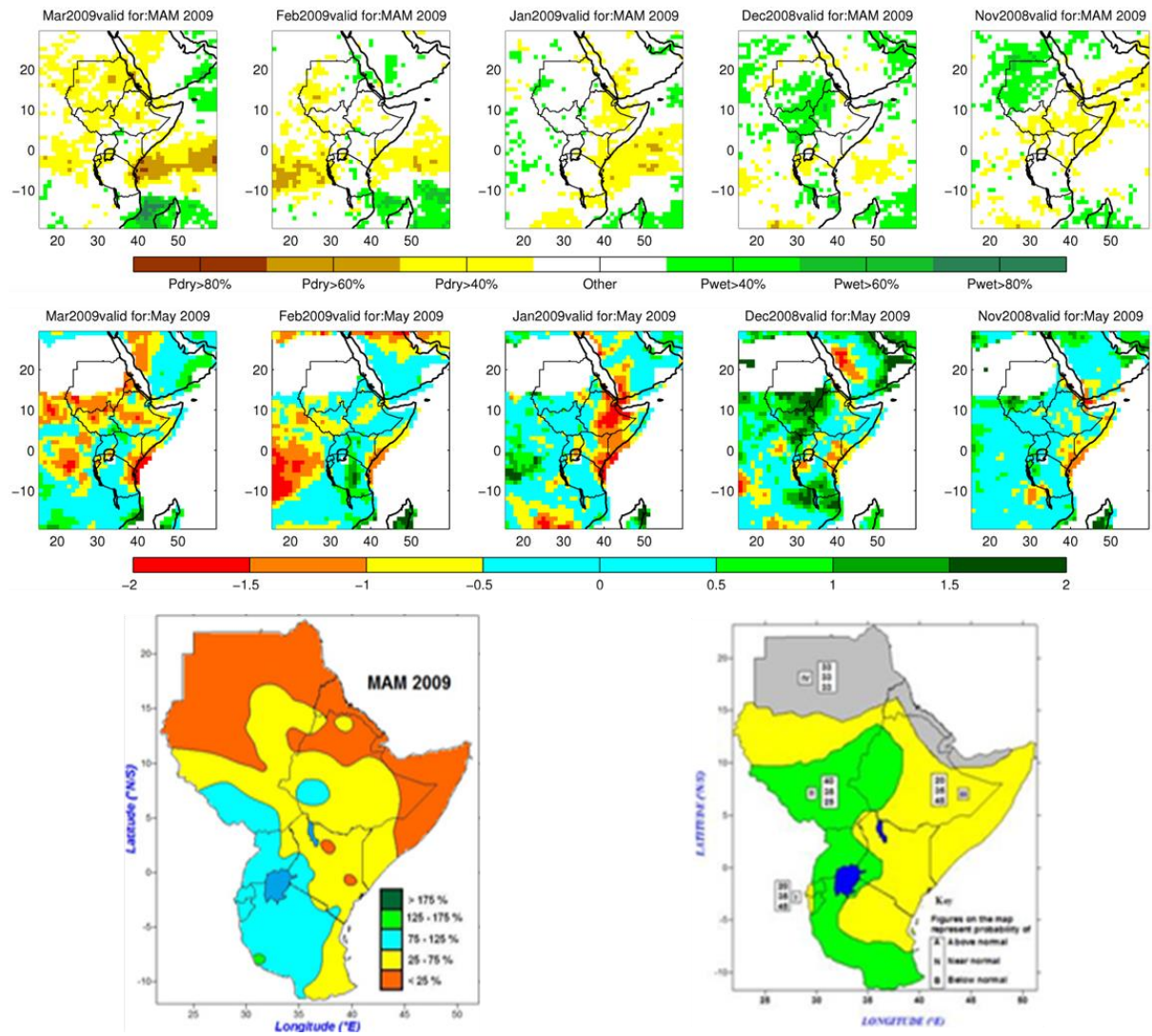


Figure 4-9 SYS-4 probabilistic precipitation forecast for 5 lead times (Top panel), SYS-4 3-month SPI forecast for 5 lead times (Middle panel), observed precipitation (Lower panel, left) and GHACOF consensus (Lower panel, right) all for MAM 2009.



5. VISUALIZATION OF THE FORECAST INFORMATION INTO THE MAP VIEWER

5.1 SYSTEM ARCHITECTURE

The Map Viewer is a web Geographic Information System (GIS) living inside the website dedicated by JRC to the DEWFORA project. The source of geographical and thematic contents used for maps and charts are: locally stored raster images and ESRI shapefiles, OGC (Open GeoSpatial Consortium) Web Map Services (WMS) layers and Oracle spatial tables.

The Map Viewer is implemented in PHP language and uses the Open Source Geospatial Foundation (OSGeo) MapServer as the GIS engine, accessed through PHP MapScript. The web interface is enhanced using Cascading Style Sheets (CSS) and JavaScript, by both homemade code and frameworks like jQuery, OpenLayers, and Flot. Several PHP classes and programs and JavaScript functions were implemented expressly to manage a sizeable amount of layers, to present contents at both continental and local scale (i.e. at the scale of a specific case study), to draw charts of the main indicators, and to compare more indicators at different dates.

In order to clearly present the user all the information, the Map Viewer has been developed with a tab structure: some tabs contain the map generated by client-server calls of MapServer aimed to detailed visualizations and queries, while the comparison and graph tabs make use of client-side technologies to provide quick overviews. Taking advantage of the PHP program that manages the content of the whole DEWFORA website, if needed it would be possible to translate the Map Viewer into different languages used in Africa.

5.2 WEB PORTAL AND FUNCTIONALITIES

The Map Viewer (<http://edo.jrc.ec.europa.eu/dewfora/php/index.php?id=4119>) is provided with a set of functionalities to display and query the data. It is organized in tabs, in order to present a continental overview (tab 1), to focus one of the project case studies (Limpopo, Niger, Nile, or Oum er-Rbia river basins; tabs from 2 to 5), or to display time series graphs of drought products (tab 6). A seventh tab hosts the comparison tool, where four so called “Side-by-Side Maps” allow to see the same indicator at four different dates, or different indicators at the same date, or all the possible combinations in between.

The main differences between the Map Viewer in the first tabs and the “Side-by-Side” tool are the core GIS technology they use and the way to present contents. The main Map Viewer is based on MapServer, while Side-by-Side Maps makes use of OpenLayers. The former has only one map with many layers and functions and is thought for detailed analyses

like a desktop GIS, while the latter is composed by four maps with basic functions only, to enhance the quick comparison of the content the four maps display.

In the following sections the different parts of the web portal and the available functionalities are described.

5.2.1 DEWFORA Map Viewer

As said before, the first tab of the Map Viewer and the similar following case study tabs are focused on the data visualization, querying and browsing.

In Figure 5-1 and Figure 5-2 it is possible to see the main structure of the Map Viewer. The graphical interface of the Map Viewer is composed by three main sections: a list of Tables of Contents (TOCs) on the left side of the page, the map on the right, and a toolbar over it.

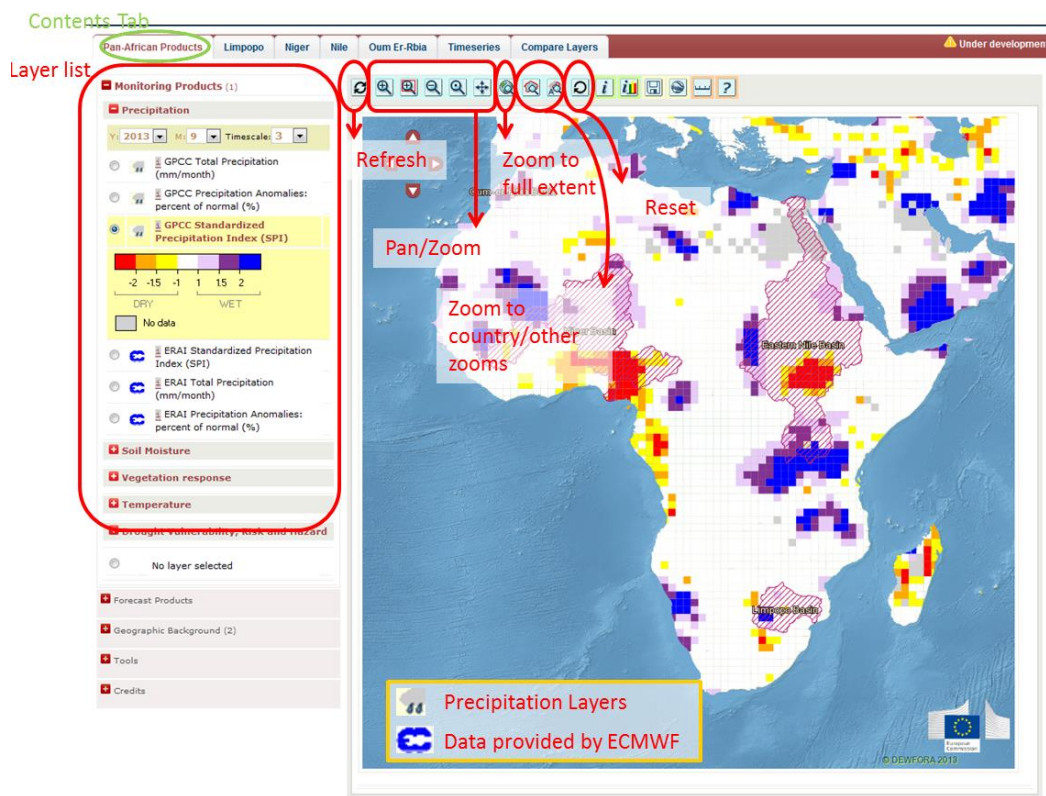


Figure 5-1 Main page of the Map Viewer. Layer list structure and Toolbar highlighted

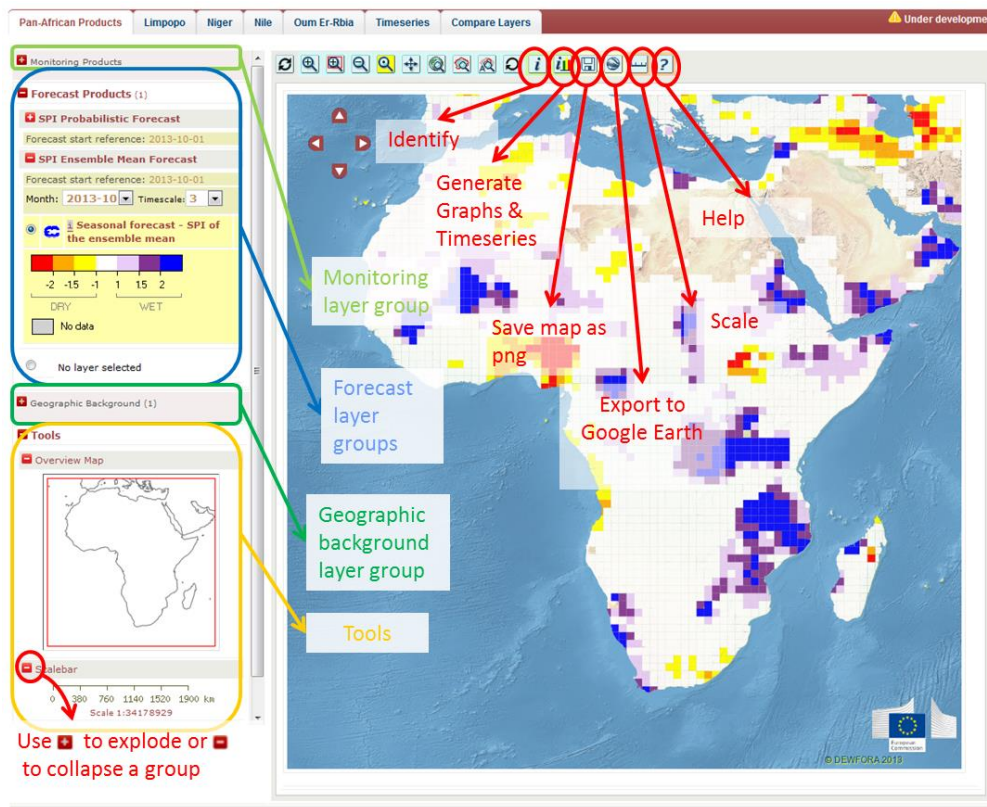


Figure 5-2 Main page of the Map Viewer. Main tools and layer groups highlighted

The TOC contains the list of layers used in DEWFORA. Since it is possible to define more than one TOC, the layers can be organized in many TOCs, representing the highest level of layer categorization.

Moreover, each TOC can contain one or more thematic group of layers (second level of categorization) and each group can be divided in three time-based subgroups (third level of categorization): “*Layer with time series*” (containing layers provided with many source images for different dates), “*Layers with last available map only*” (layers coming with only the source image referring to the last available date), and “*Layers without time series*” (layers not considering time). “*Layers with time series*” has also different dropdown menu to select the reference period that can be a full date or a combination of the values of year, month and ten-day period menus (see Figure 5-3). A dropdown menu to select a timescale is available too (e.g. for SPI layers). Each layer name is presented with a control (radio button or checkbox) to activate or deactivate it, the legend (at the left or below the layer name), a button to switch the legend on/off if it is too long and an “info box (i)” to display the layer description.

The drought related information in the TOC is divided in four main themes:

1) Monitoring Products: a real-time monitoring system containing precipitation, temperature, soil moisture, and their anomalies (including the so-called Standardized Precipitation Index –

SPI). Historical monthly data and products are available for visualization starting from 1979 to present for ERA-Interim data, while the GPCP (Global Precipitation Climatology Centre) precipitation products are available from 1950 onwards.

2) Forecast Products: seasonal forecasts of Standardized Precipitation Index (SPI) using GPCP and ERA Interim precipitation merged with the ECMWF Seasonal Forecast system 4 up to 7 months (from 1 to 7 months forecast) taking into account the month of issue.

3) Vulnerability and Risk analysis: Drought Hazard, Vulnerability and Risk maps are presented at country level and river basin scale.

4) Geographic background: allows visualizing a set of ancillary layers.

Below the layer list, the overview map and the scale bar are shown (see Figure 5-2).

In the case of Forecast Products, the user can visualize in the TOC menu the date of forecast and then it is possible to select among the following seven forecasted months and the available aggregation period of SPI (see Figure 5-4).

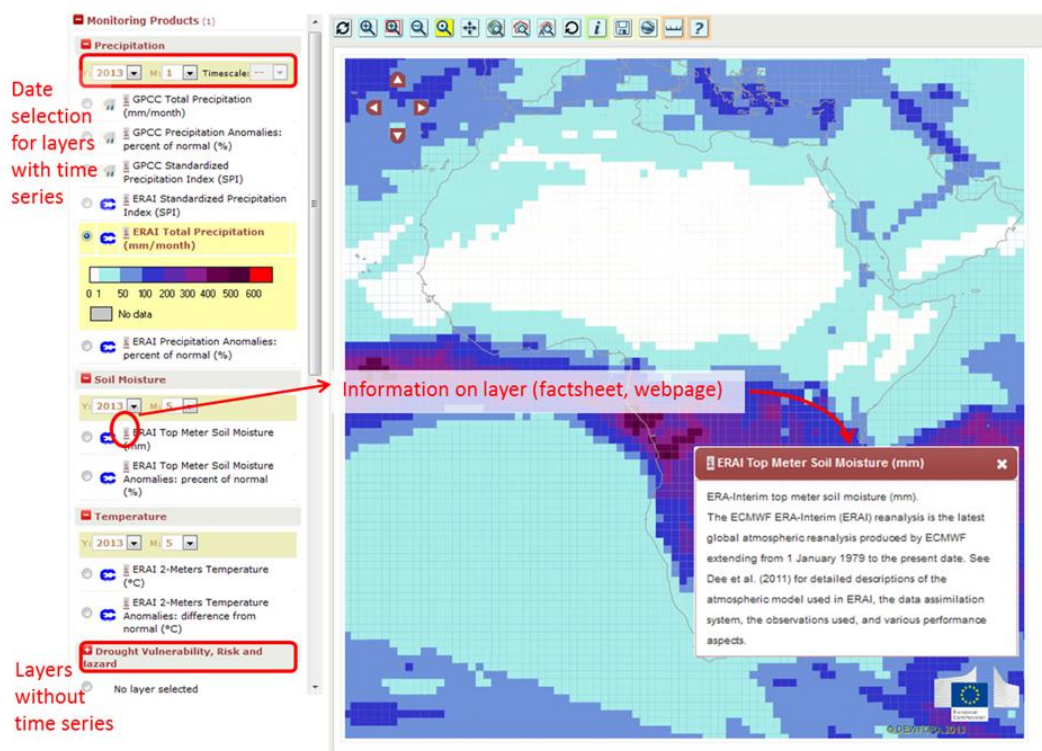


Figure 5-3 Layer time selection and information visualization

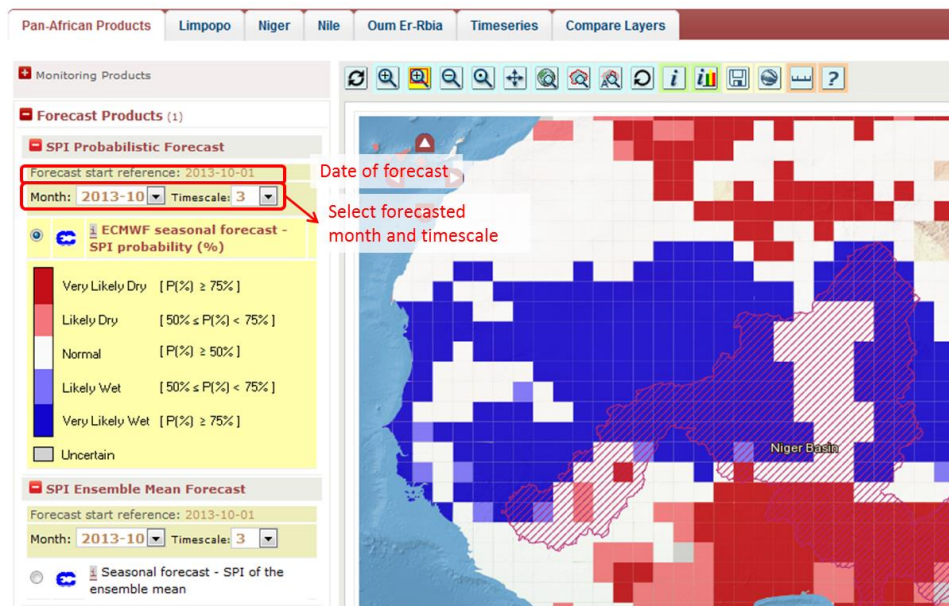


Figure 5-4 Date selection for forecasting layers

The **toolbar** of DEWFORA contains many icons to exploit different functions. Figure 5-1 and Figure 5-2 and the list below sum them up:

- **Reload/Refresh** and **Zoom to Layer**: clicking the icon the map is re-drawn taking care of new settings, i.e. new geographical extent, activation/deactivation of layers, or selection of different reference dates. When a layer is newly activated or deactivated, the button “Refresh map”, hidden by default, is displayed: clicking on it, a map refresh is invoked. Moreover, if the layer is provided with the “Zoom to layer” property, also the button “Zoom to layer” (hidden by default too) appears and the action associated to it is a map refresh with the geographical extent set to the layer’s extent.
- **Standard navigation tools**: they include tools activated by clicking the corresponding icon and acting on the map: “Zoom In”, “Zoom Out”, and “Re-centre” are triggered clicking a point on the map; “Zoom Rectangle” is executed by drawing a rectangle on the map, “Pan” requires that the user drags and moves the map.
- **Full Extent** extends the map to the maximum extent allowed for DEWFORA.
- **Zoom to Country** opens a select menu where the user can choose the country which the map must be zoomed to. **Other Zooms** first proposes the list of available zooms; then, when a zoom is selected, displays a list of features to zoom to, pre-filtered by letter or by country. At the moment the two other zooms available are “Go to town” and “Zoom to river basin”. “Zoom to” usually applies to polygons and lines and redraw the map with the geographical extent corresponding to the bounding box of the selected feature. Instead, “Go to” applies to points and centres the map in the selected punctual feature. The scale is not changed, unless it is greater than a pre-defined threshold, set to 1:10000000. In this case the new map scale is set to this value.

- **Reset:** clicking the icon, the map is re-drawn at the initial visualization.
- **Identify:** this function allows users to query the map, by clicking on it and retrieving results for the selected layers at the clicked coordinates. Technically, the clicked coordinates are used for a spatial query of the Oracle table underlying the selected layer. After activating this function by clicking the proper icon (1 in Figure 5-5), a new line is displayed under the toolbar. Here the user can choose which layer to query (2 of Figure 5-5) and to highlight the selected feature on the map. For subsequent queries, it is possible to perform a new query in the point of the previous one by clicking the specific button. Identified results are displayed in a floating table (3 in Figure 5-5). Each variable is a row in the table and can be provided with “Generate KML” tool to export the geometry of the feature in KML (Keyhole Markup Language) format and display it in a third party software like Google Earth.

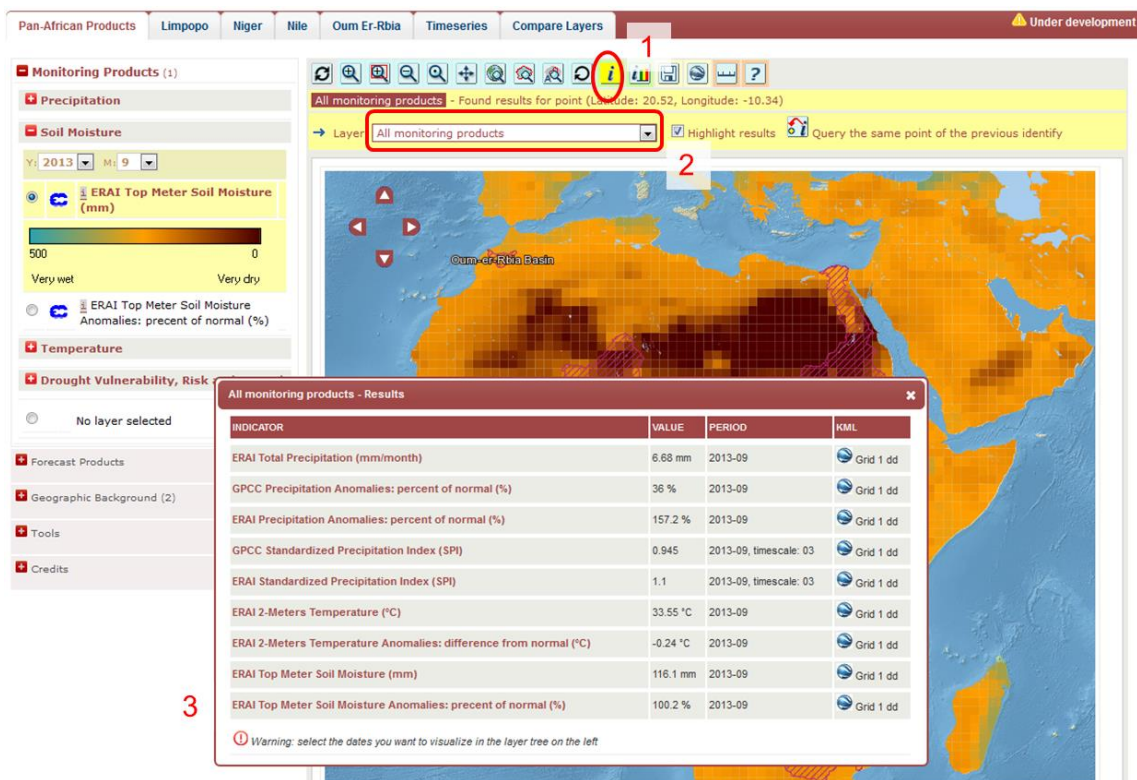


Figure 5-5 Identify function example

- **Generate graphs and time series:** Here the user can click a point on the map to set the location where the graph must be drawn or directly click on the link to draw it for the map centre. (See Section 5.2.2 for further details).
- **Export:** it's possible to export the map content, saving the whole map as PNG image using “Export PNG from Current View” or as KML Ground Overlay using “Export KML for Google Earth”.



– **Help:** the icon opens the web page of Map Viewer Help.


–

5.2.2 DEWFORA Time Series

The sixth tab of the DEWFORA Map Viewer, named **Time series**, contains the **Unified Graph Creator (UGC)**, a tool written in PHP and using Flot (see <http://www.flotcharts.org>), a plotting library for jQuery.

It is aimed to display a graph of one or more drought indicators for the selected period at a given point on Earth, as shown in Figure 5-6.

Users can set the graph location writing its latitude and longitude in the text fields (see box 1 of Figure 5-6), the time interval selecting the first and the last year (box 2), the drought indicators marking the correspondent checkboxes (box 3), and, optionally, a title and subtitle for the graph writing it the specific text field (box 4).

The graph generation is triggered by the “**Draw graph**” button, highlighted in box 5 of Figure 5-6 together with the “**Reset**” button and the  icon that opens the UGC help page.

Generated graph has the following properties:

- time is presented in the horizontal axis;
- each indicator has its own vertical axis;
- vertical axes of the same indicators provided by different subjects (e.g. GPCC Rainfall and ERAI Rainfall) are synchronized, i.e. they have coincident ordinates;
- a legend of indicators and their units of measurement is displayed on the top-left corner (see box 6 of Figure 5-6)
- a tooltip shows the plotted value when it is overpassed by the mouse (box 7)
- if provided, the title is written at the top of the graph;
- it's possible to draw a rectangle on the graph and zoom on it (see boxes 15 and 16 of Figure 5-7) and return to the initial extent clicking the button “**Reset zoom**” (box 17).

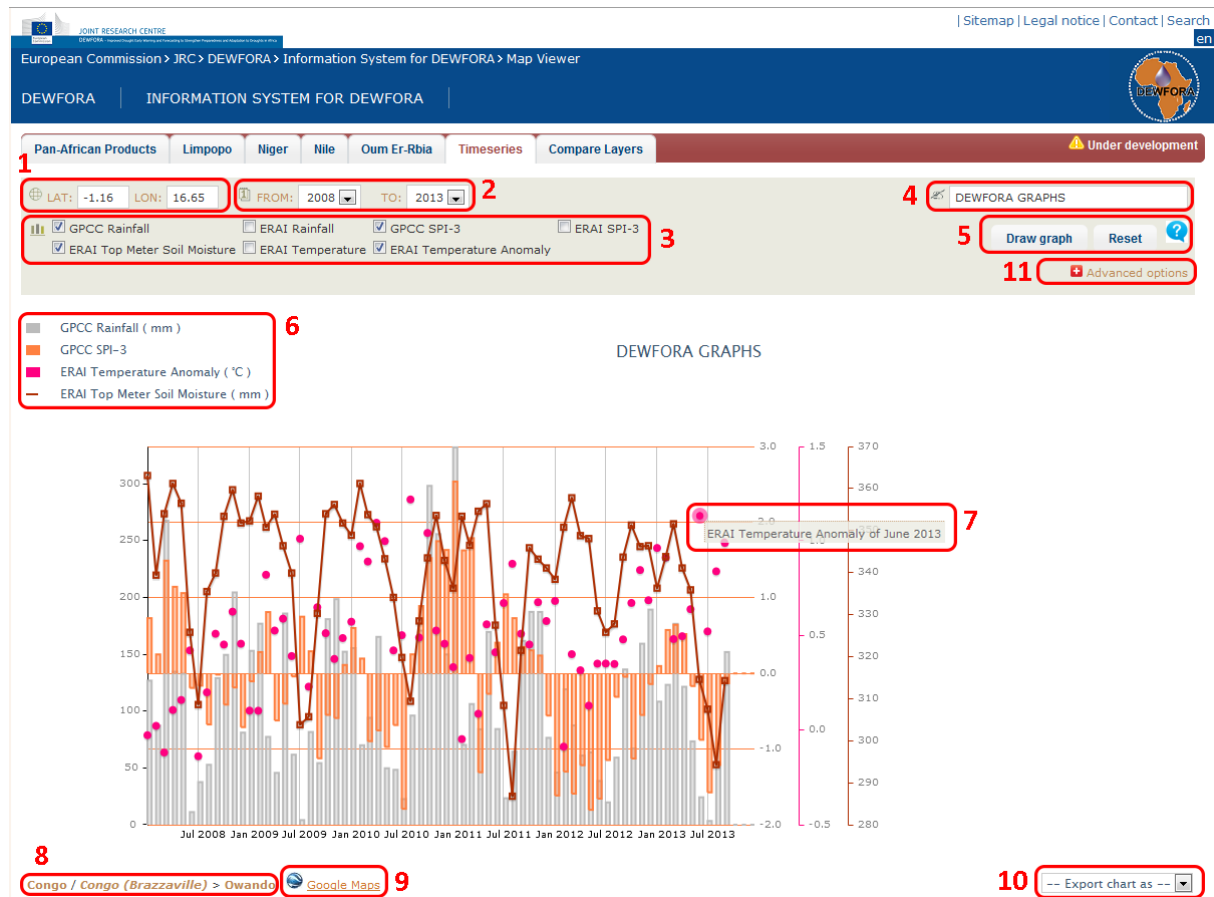


Figure 5-6 Graph of GPCC Rainfall, GPCC SPI-3, ERA1 Top Soil Moisture, and ERA1 Temperature Anomaly from 2008 to 2013, drawn at the point with Lon 16.65 and Lat -1.16

Three tools displayed under the graph provide additional functionalities:

- **Nearest location** (box 8 of Figure 5-6): the town closest to the given coordinates is stated;
- **Google Maps** (box 9): clicking this link it's possible to centre Google Maps in the given point;
- **Export** (box 10): with this function it's possible to save the graph as PDF document or as PNG or JPEG image.

The following **Advanced options** are also available in UGC and can be visualized by clicking the button highlighted in box 11 of Figure 5-6):

- **Location by Town** (box 12 of Figure 5-7): menus to select a town whose coordinates will be used as graph location;
- **Subtitle** (box 13): text field to set a subtitle that will be visualized in the graph below the title;
- **Graph colours** (box 14): list of colours to be used for plotting graph lines, points and histograms instead of the default colours.

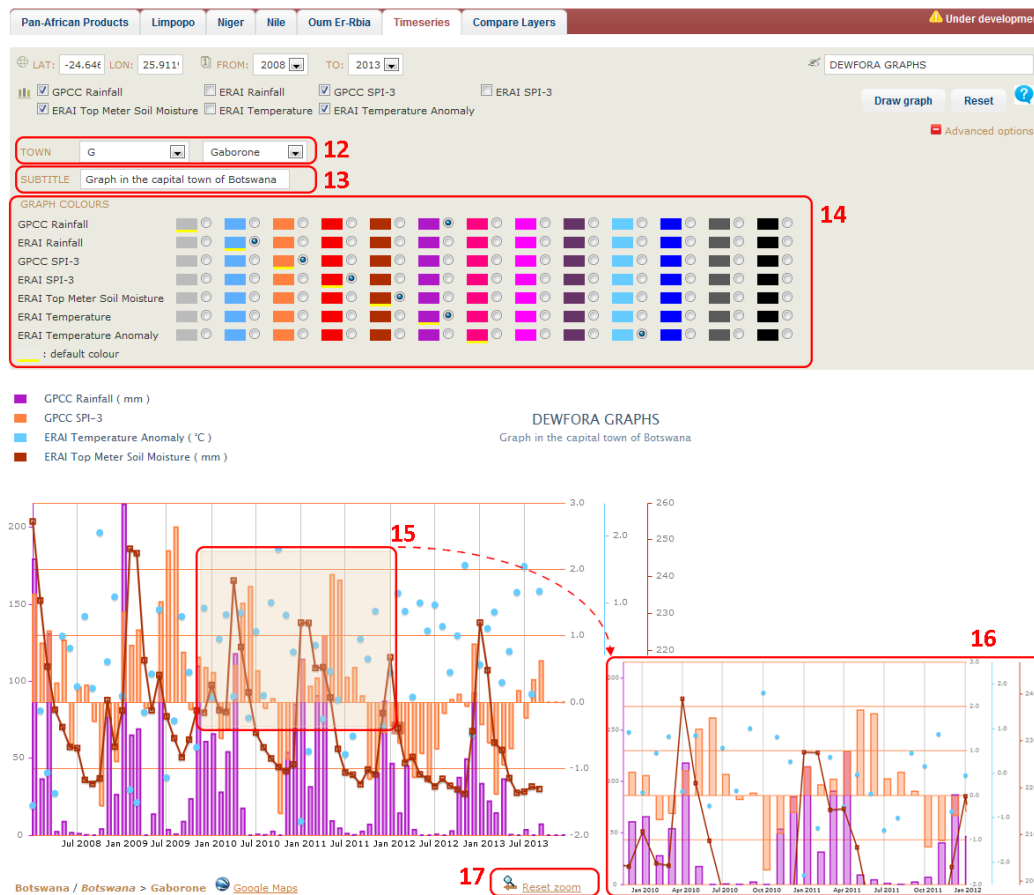


Figure 5-7 Use of UGC advanced options: in the example the town of Gaborone is used to set the coordinates of the graph location, optional colours are set for GPCC Rainfall and ERAI Temperature Anomaly, and a subtitle is present. Moreover, the image shows the zoom.

The UGC of DEWFORA can be opened both from the tabs themselves, as described in paragraph 5.2.1, and from the website menu, hence independently from the Map Viewer.

5.2.3 DEWFORA Compare Layers

The last tab of the DEWFORA Map Viewer is named **Compare Layers** and allows comparing different indicators simultaneously, action otherwise impossible or unclear just overlying the layers of those indicators in the same map.

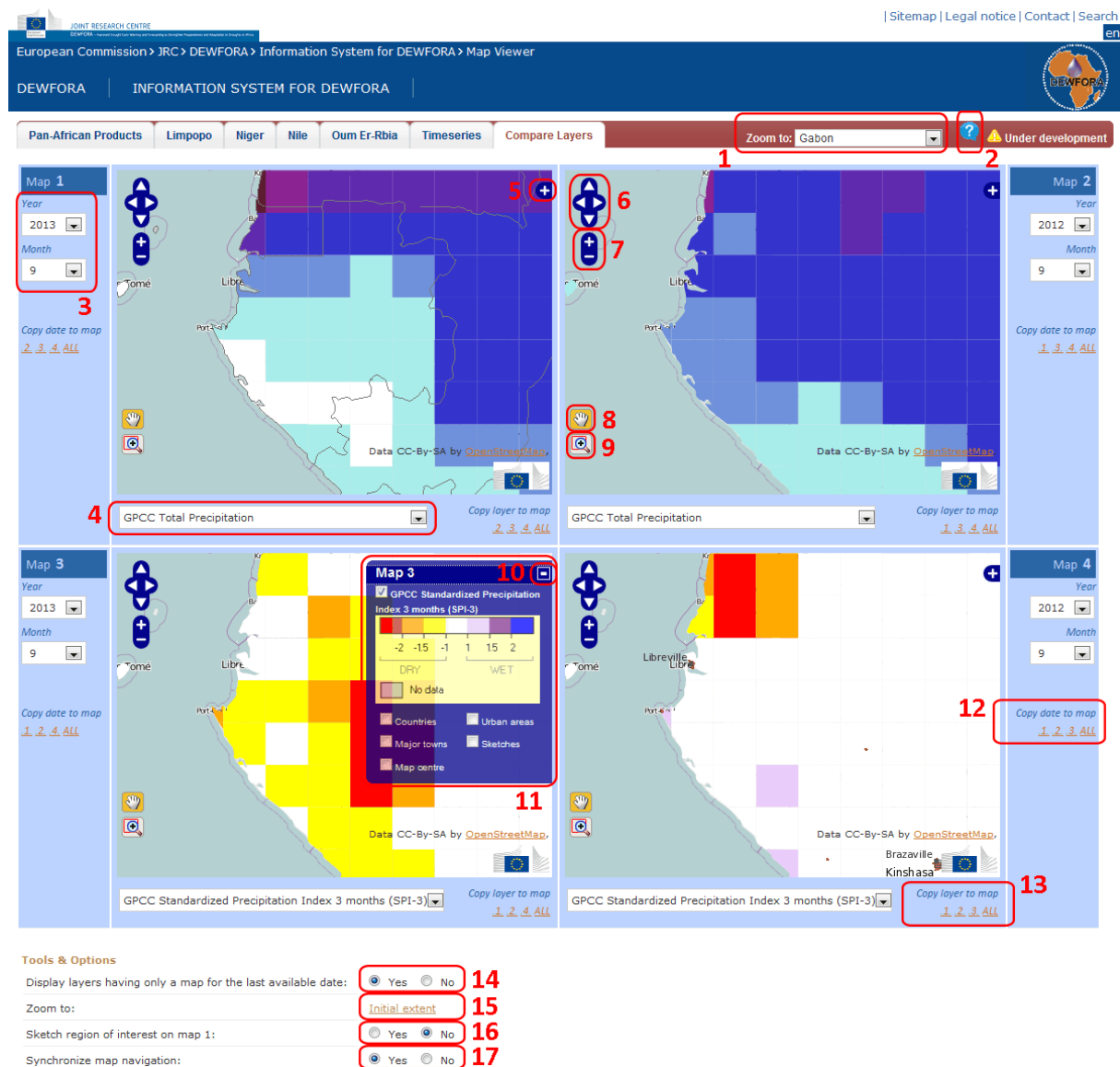
The comparison is made possible by four synchronized maps, where users can select the indicator and its reference date. **Side-by-Side Maps (SBSM)** is the name assigned to these four maps tool and to the program to manage them, implemented in PHP and JavaScript and it uses the OpenLayers library and WMS services.

In SBSM it is possible to perform two important analyses to study a drought event and its evolution: comparing four different indicators (an indicator for each map) at the same time or comparing the same indicator at four different times (a different time for each map). Since any indicator and date can be selected in each map independently from the others, all the

combinations in between are possible. For example, the Figure 5-8 shows GPCC Total Precipitation in the top maps and GPCC SPI-3 in the bottom ones, while the date is September 2013 in the left maps and September 2012 in the right ones.

Moreover, the navigation of the four maps is synchronized by default. This means that when users do zoom or pan in a map, all the other maps are zoomed or panned to the same geographical extent.

SBSM provides also other map and global properties and functions, as detailed in the next lines.



The screenshot displays the DEWFORA Information System for DEWFORA Map Viewer interface. The interface is divided into several sections:

- Navigation Bar:** Includes tabs for 'Pan-African Products', 'Limpopo', 'Niger', 'Nile', 'Oum Er-Rbia', 'Timeseries', and 'Compare Layers'. A 'Zoom to: Gabon' dropdown is present, along with a 'Under development' warning.
- Map Grid:** Four maps are displayed in a 2x2 grid:
 - Map 1:** GPCC Total Precipitation for September 2013.
 - Map 2:** GPCC Total Precipitation for September 2012.
 - Map 3:** GPCC Standardized Precipitation Index 3 months (SPI-3) for September 2013.
 - Map 4:** GPCC Standardized Precipitation Index 3 months (SPI-3) for September 2012.
- Left Sidebar:** Contains date selection (Year: 2013, Month: 9) and a 'Copy date to map' button.
- Map 3 Legend:** A legend for 'GPCC Standardized Precipitation Index 3 months (SPI-3)' is displayed, showing a color scale from -2 (Dry) to 2 (Wet), with 'No data' in grey. It also includes options for 'Countries', 'Urban areas', 'Major towns', and 'Map centre'.
- Tools & Options:** Located at the bottom, it includes:
 - 'Display layers having only a map for the last available date:' with radio buttons for 'Yes' (selected) and 'No'.
 - 'Zoom to:' with a dropdown set to 'Initial extent'.
 - 'Sketch region of interest on map 1:' with radio buttons for 'Yes' and 'No' (selected).
 - 'Synchronize map navigation:' with radio buttons for 'Yes' (selected) and 'No'.

Figure 5-8 Compare Layers: GPCC Total Precipitation and GPCC SPI-3 in September 2012 and September 2013 over Gabon. The legend is displayed only in one of the four maps.

- **Selection of the indicator** to be loaded in a map (see box 4 of Figure 5-8): indicators are presented in a selection list, where indicators that have associated different



aggregation period (e.g. SPI) have a single entry for each aggregation period (e.g. GPCC SPI has seven entries because it has seven timescales).

- **Selection of the indicator's reference date** for that map (box 3); at the moment there are indicators that are updated monthly.
- **Navigation tools**: pan (box 8), zoom in/out (7), zoom to North/South/East/West (6), and zoom by rectangle (9). When the synchronization of map navigation is enabled, a pan or a zoom action on a map triggers the same action on the others; otherwise, if the synchronization of map navigation is disabled, a pan or a zoom action on a map applies on that map only.
- **Legend** of layers available for a map (box 11); the legend is hidden by default and can be switched on or off by means of a button in the top-right corner of the map (boxes 5 and 10 respectively).
- **Copy date to maps**: with one of the buttons of box 12 it's possible to set the date of a map in another map or in all the maps.
- **Copy layer to maps**: with one of the buttons of box 13 it's possible to set the indicator of a map in another map or in all the maps.

All these map properties are invoked in a single map and can affect that single map only or all the maps.

The global properties of SBSM affect the tool itself and apply to all the maps simultaneously; they are:

- Possibility to **enable/disable the synchronization of map navigation** (box 16 of Figure 5-8);
- **Zoom to**: it's possible to do zoom to a predefined geographical extent among the whole continent, the four case study areas, all African countries (all selectable by the menu shown in box 1), and the initial extent (box 15).
- Possibility to enable/disable the **display of layers having only a map for the last available date** and not a complete time series (box 14).
- **SBSM Help page**, opened by the icon highlighted in box 2.
- **Sketch region of interest on map 1**: it's possible to sketch a region of interest in map 1 (top-left map) and automatically see it also on the other maps. This tool is useful to detect and highlight an affected area in map 1 and check in the other maps if the same area is affected also in other dates and/or according to other indicators. The tool is enabled by the radio button highlighted in box 20 of Figure 5-9 and consists of the editing toolbar highlighted by box 17 and useful to sketch a polygon, a line, or a point on the map. For example, in Figure 5-9 an affected area by drought has been detected and drawn among South Sudan, Democratic Republic of the Congo and Uganda (box 18) on the map of GPCC SPI-3 of June 2013. That region of

interest is automatically displayed in the other maps, where users can study the impact of different variables in the same area as ERAI 2-Meters Temperature Anomalies (map 3, bottom-left), and if it was already affected in the GPCCC SPI-3 map of the previous month (map 2, top-right), and if the situation was present also in the previous year (map 4, bottom-right). The regions of interest sketched by the users can be toggled on and off in the map like a normal layer (box 19) or permanently deleted in one or all the maps (box 21).

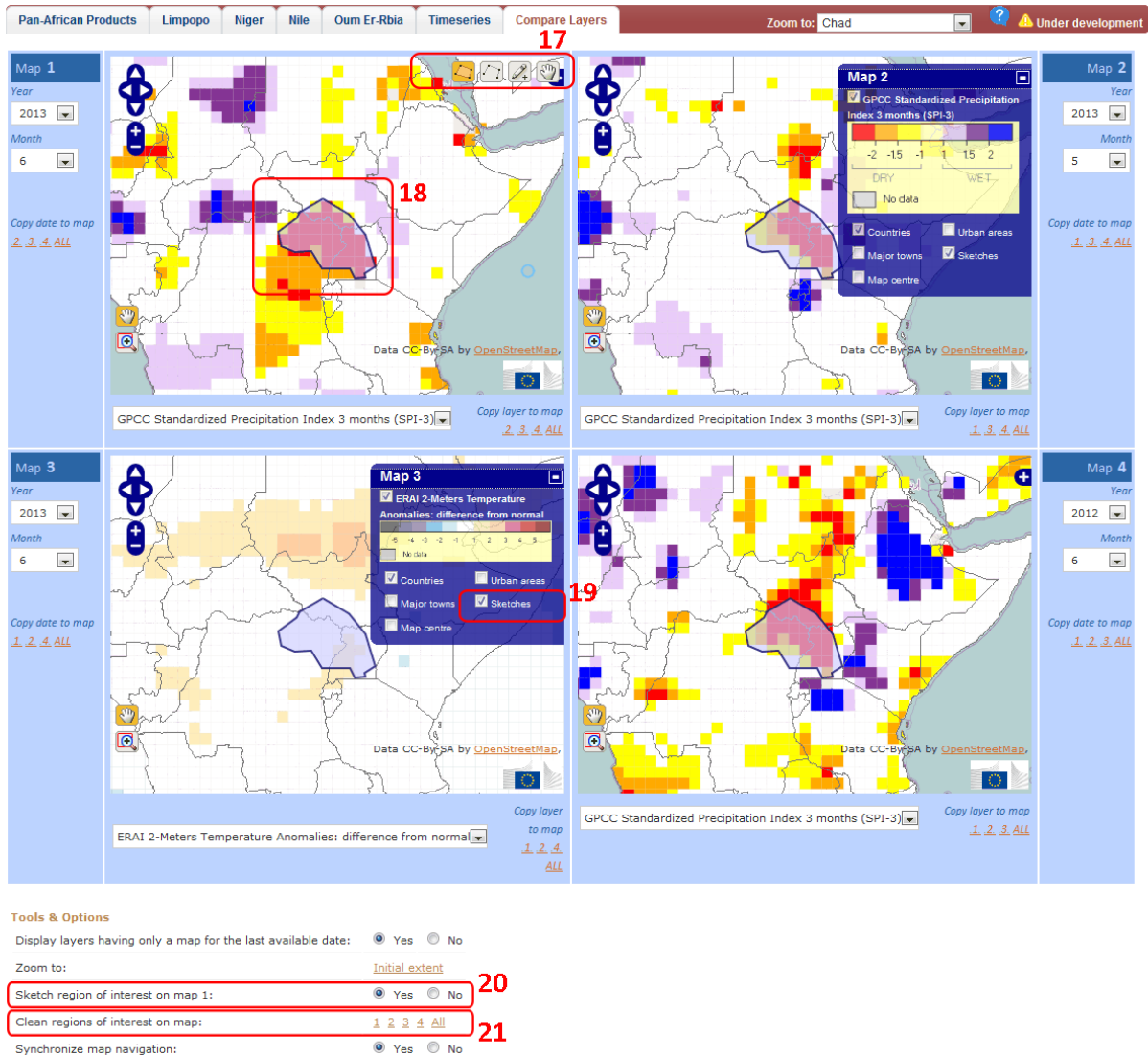


Figure 5-9 Compare Layers: Example of sketching an affected area in map 1 and checking if it is detectable also in the other maps, where a different indicator (bottom-left map) or different dates (right maps) have been selected.



6. CONCLUSIONS

This report presents the methodology and initial verification of an integrated global drought monitoring and seasonal forecast system. The verification results clearly identified the regions and Standard Precipitation Index (SPI) time-scales that benefit from using dynamical model precipitation forecasts as compared with climatological precipitation forecasts. These regions are mainly located in the tropical area where climatic signals, such as ENSO, provide long-term predictability. For the SPI-3 in Northern Europe there is no benefit in using the S4 forecasts, while in all the remaining regions the S4 forecasts are beneficial. For the SPI-6 the use of S4 forecasts in Northern Europe and Central America also do not bring any added value to the climatological forecasts. For the SPI-12 this is also the case for the entire North America, North Eurasia, East Africa and Australia.

The results over Africa, and in particular over South Africa, are very encouraging for further developments of the proposed integrated drought monitoring and seasonal forecasts system and its integration within the map viewer. These results show that this system has the potential to provide skilful information to end-users, but such information needs to be carefully delivered, in particular recognizing its limitations in terms of skill. Another point that should be addressed is the difference between statistically significant skill and useful skill. This will require a close collaboration with end-users to identify what are the acceptable levels of skill for their particular applications.

In this report we have also analysed if the availability of long range forecasts from ECMWF and the use of more specific drought indicators such as the SPI would bring any added benefits to the Greater Horn of Africa Climate Outlook Forums. As a first step ECMWF seasonal precipitation forecasts (S4) were evaluated against station data over a vast part of the Great Horn of Africa using the historical datasets which are also the reference for the consensus climatology. Considering the paucity of data in this area and the difficulty to obtaining a long term dataset, this by itself has represented a reality check of the performances of the system in a critical region for drought monitoring. S4 has significant skill in forecasting precipitation over East African with remarkably high skill in predicting the short rains (October-December) due to the strong predictability of the Sea Surface Temperature in the Indian Ocean and the ENSO teleconnection (Hastenrath et al., 2004). The good performance of the system over the region is a good starting point; nevertheless the interest here is in understanding if the availability of frequent updates from a dynamical model would add useful information to the already existing forecaster's interpretation of the statistical forecasts. While the subjective assessment showed that there would be an added value, no particular lead time stood out in provision of more information for the entire period but in each season there was a lead time that would have made the consensus forecast better. The most



interesting result is that if SPI is used in place of raw precipitation to generate a “proxy” of the consensus maps, then not only do the maps become spatially homogeneous but information about the intensity of the conditions expected in the next season are available. Such information could then be used to support the decision process when issuing advisories for policy actions within the region.

The Pan-African Map Viewer integrated drought monitoring and seasonal forecasting related information in an innovative approach for Africa, following a similar system developed for Europe through the European Drought Observatory. Such a monitoring and forecasting system provides multiple drought meteorological and hydrological products with vulnerability and risk maps derived from socio-economic indicators. This information can be a useful input for existing and future drought early warning systems since it provides information on drought magnitude and extent, as well as understanding the potential drought impacts. Although the system is still under development it is already in a demonstration pre-operational phase, with a variety of tools and drought related products that are accessible to end users and stakeholders interested in drought information in Africa.



7. REFERENCES

- Balsamo, G., Bousetta, S., Lopez, P. and Ferranti, P., 2010.: Evaluation of ERA-Interim and ERA-Interim-GPCP-rescaled precipitation over the U.S.A., ECMWF, Reading. [online] Available from: <http://www.ecmwf.int/publications/library/do/references/show?id=89966> (Accessed 2 August 2011).
- Beltrando, G., 1990: Space-time variability in April and October-November over East Africa during the period 1932-1983. *International Journal of Climatology*, 10, 691-702
- Bierkens, M. F. P. and Van Beek, L. P. H., 2009: Seasonal Predictability of European Discharge: NAO and Hydrological Response Time, *Journal of Hydrometeorology*, 10(4), 953–968, doi:10.1175/2009JHM1034.1.
- Candogan Yossef N, van Beek LPH, Kwadijk JCJ, Bierkens MFP, 2011: Skill assessment of a global hydrological model in reproducing flow extremes. *Hydrol Earth Syst Sci Discuss* 8: 3469-3505
- Dee, D. P., et al., 2011: The ERA-Interim reanalysis: Configuration and performance of the data assimilation system. *Quarterly Journal of the Royal Meteorological Society* 137, 656, 553-597.
- DEWFORA D3.2, 2012: Methods for mapping drought vulnerability at different spatial scales. <http://www.dewfora.net/Publications>
- DEWFORA D4.2, 2011: Skill of the multi-model forecasting system in predicting variables and drought indicators. <http://www.dewfora.net/Publications>
- DEWFORA D4.3, 2012: Potential to supplementing drought early warning systems with new meteorological information. <http://www.dewfora.net/Publications>
- DEWFORA D4.5, 2011: Available continental scale hydrological models and their suitability for Africa. <http://www.dewfora.net/Publications>
- DEWFORA D6.3, 2012: Testing of drought indicators at Pan-African level. <http://www.dewfora.net/Publications>
- DEWFORA D6.4, 2013: Integration of Drought Vulnerability and Hazards into Risk maps at the Pan-African level. <http://www.dewfora.net/Publications>
- Droogers, P. and Allen, R., 2002: Estimating Reference Evapotranspiration Under Inaccurate Data Conditions, *Irrig. Drain. Syst.*, 16, 33–45.
- Dutra, E., Giuseppe, F. D., Wetterhall, F., and Pappenberger, F., 2013a: Seasonal forecasts of droughts in African basins using the Standardized Precipitation Index. *Hydrology and Earth System Sciences*, 17(6), 2359-2373.
- Dutra, E., Magnusson, L., Wetterhall, F., Cloke, H. L., Balsamo, G., Bousetta, S., & Pappenberger, F., 2013b: The 2010–2011 drought in the Horn of Africa in ECMWF reanalysis and seasonal forecast products. *International Journal of Climatology*, 33, 7, 1720–1729.
- Dutra E., F. Wetterhall, F. Di Giuseppe, G. Naumann, P. Barbosa, J. Vogt, W. Pozzi, and F. Pappenberger, 2013c: Global meteorological drought: Part I - probabilistic monitoring. Submitted to *Hydrol. Earth Syst. Sci.*
- Edwards, D.C. and McKee, T. B., 1997: Characteristics of 20th century drought in the United States at multiple time scales. *Climatology Report Number 97-2*, Colorado State University, Fort Collins, Colorado



- Giorgi, F., and Francisco, R., 2000: Uncertainties in regional climate change prediction: a regional analysis of ensemble simulations with the HADCM2 coupled AOGCM, *Climate Dyn.*, 16, 169–182, 10.1007/pl00013733.
- Hargreaves, G. H. and Allen, R. G., 2003: History and Evaluation of Hargreaves Evapotranspiration Equation, *J. Irrig. Drain. E.-ASCE*, 129, 53–63, 2003.
- Hastenrath, S., Polzina, D. and Camberlin, P., 2004: Exploring the Predictability of the ‘Short Rains’ at the Coast of East Africa. *Int. J. Climatol.* , 24, 1333–1343
- Hersbach, H., 2000: Decomposition of the continuous ranked probability scores for ensemble prediction systems. *Weather and Forecasting*, 15(5), 559–570
- Hollingsworth, A., Arpe, K., Tiedtke, M., Capaldo, M. and Savijärvi, H., 1980: The performance of a medium-range forecast model in winter impact of physical parameterizations. *Mon. Weather Rev.*, 108, 1736–1773
- Mason, S. J. and Graham, N. E., 2002: Areas beneath relative operating characteristics (ROC) and relative operating levels (ROL) curves: Statistical significance and interpretation. *Q. J. R. Meteorol. Soc.*, 128, 2145–2166
- Mckee, T. B., Doesken, N. J., and Kleist, J., 1993: The relationship of drought frequency and duration to time scales. Eight Conference on Applied Climatology, Anaheim, California, 179-184
- Miyakoda, K., Hembree, G. D., Strickler, R. F. and Shulman, I., 1972: Cumulative results of extended forecast experiments. Model performance for winter cases. *Mon. Wea. Rev.*, 100, 836-855
- Molteni, F., Stockdale, T., Balmaseda, M., BALSAMO, G., Buizza, R., Ferranti, L., Magnunson, L., Mogensen, K., Palmer, T., and Vitart, F., 2011: The new ECMWF seasonal forecast system (System 4), ECMWF Tech. Memo., 656, 49 pp.
- Mutai, C.C., Ward, M.N. and Coleman, A.W., 1998: Towards the prediction of the East Africa short rains based on sea-surface temperature-atmosphere coupling. *International Journal of Climatology*, 18, 975-997
- Naumann, G., Barbosa, P., Carrao, H., Singleton, A., and Vogt, J. 2012: Monitoring Drought Conditions and Their Uncertainties in Africa Using TRMM Data. *Journal of Applied Meteorology and Climatology*, 51(10), 1867-1874.
- Naumann G., Dutra E., Barbosa P., Pappenberger F., Wetterhall F, and Vogt J., 2013a: Establishing the dominant source of uncertainty in drought indicators. *Hydrol. Earth Syst. Sci. Discuss.*, 10, 13407-13440, doi:10.5194/hessd-10-13407-2013.
- Naumann, G., Barbosa, P., Garrote, L., Iglesias, A., and Vogt, J., 2013b: Exploring drought vulnerability in Africa: An indicator based analysis to inform early warning systems. *Hydrol. Earth Syst. Sci. Discuss.*, 10, 12217-12254, doi:10.5194/hessd-10-12217-2013.
- Nicholson, S.E. and Nyenzi, B.S., 1990: Temporal and spatial variability of SSTs in the tropical Atlantic and Indian Oceans. *Meteorology and Atmospheric Physics*, 42, 1-17
- Nicholson, S. E., 1996: A review of climate dynamics and climate variability in Eastern Africa. *The climatology and paleoclimatology of the East African lakes*, 25-56
- Nicholls, N., 1999: Cognitive illusions, heuristics, and climate prediction. *Bull. Amer. Meteor. Soc.*, 80, 1385–1398.
- Ogallo, L.J., 1982: Quasi-periodic patterns in the East Africa rainfall records. *Kenya Journal of Science and Technology*, A3, 43-54



- Ogallo, L.J., Janowiak, J.E. and Halpert, M.S., 1988: Teleconnection between seasonal rainfall over East Africa and Global seas surface temperature anomalies. *Journal of the Meteorological Society of Japan*, 66, 807-822
- Ogallo, L., Bessemoulin, P., Ceron, J. P., Mason, S., & Connor, S. J., 2008: Adapting to climate variability and change: the Climate Outlook Forum process. *Bulletin of the World Meteorological Organization*, 57(2), 93-102.
- Palmer, T., Buizza, R., Hagedorn, R., Lawrence, A., Leutbecher, M., and Smith, L., 2006: Ensemble prediction: A pedagogical perspective, *ECMWF Newsletter*, 106, 10-17.
- Schneider U, Becker A, Finger P, Meyer-Christoffer A, Rudolf B, Ziese M, 2011: GPCP Full Data Reanalysis Version 6.0 at 1.0°: monthly land-surface precipitation from rain-gauges built on GTS-based and historic data. doi: 10.5676/DWD_GPCP/FD_M_V6_100.
- Simmons, A. J., 1986: Numerical prediction: Some results from operational forecasting at ECMWF. *Adv. Geophys.*, 29, 305–338
- Sperna Weiland FC, van Beek LPH, Kwadijk JCJ, Bierkens MFP (2010) The ability of a GCM-forced hydrological model to reproduce global discharge variability. *Hydrology and Earth System Sciences* 7: 37
- Spinoni, J., Vogt, J., Naumann, G., Carrao, H, Barbosa, P., 2013: Global climate shifts from 1951-1980 to 1981-2010 using the Köppen-Geiger classification and FAO aridity index. A focus on areas at risk of desertification. Submitted to *International Journal of Climatology*.
- Trambauer, P, E. Dutra, S. Maskey, M. Werner, F. Pappenberger, L. P. H. van Beek, and S. Uhlenbrook, 2013: Comparison of different evaporation estimates over the African continent, under review *HESSD*, 10, 8421–8465.
- van Beek, L. P. H. & M. F. P. Bierkens. 2009: *The Global Hydrological Model PCR-GLOBWB: Conceptualization, Parameterization and Verification*. Utrecht, The Netherlands: Utrecht University, Faculty of Earth Sciences, Department of Physical Geography.
- Van Beek, L. P. H., Wada, Y. and Bierkens, M. F. P., 2011: Global monthly water stress: 1. Water balance and water availability, *Water Resour. Res.*, 47(7), W07517, doi:10.1029/2010WR009791.
- Werner M, van Dijk M, Schellekens J. 2004: DELFT-FEWS: an open shell flood forecasting system. In 6th International Conference on Hydroinformatics, LiangSY, PhoonK, BabovicV (eds). World Scientific Publishing Company: Singapore; 1205–1212.
- Wesseling, C. G., Karssenber, D.-J., Burrough, P. A. and Van Deursen, W. P. A., 2008: Integrating dynamic environmental models in GIS: The development of a Dynamic Modelling language, *Transactions in GIS*, 1(1), 40–48, doi:10.1111/j.1467-9671.1996.tb00032.x, 1996. Wood, A. W. and Lettenmaier, D. P.: An ensemble approach for attribution of hydrologic prediction uncertainty, *Geophysical Research Letters*, 35(14), n/a–n/a, doi:10.1029/2008GL034648.
- World Meteorological Organisation (WMO), 2009; Press report December 2009, WMO No. 872.



8. APPENDIX I – OVERVIEW AND DEVELOPMENT OF DEWFORA MAP VIEWER PRODUCTS

The Pan-African Map Viewer relies on several variables and indicators that are relevant for drought monitoring, forecasting and decision making (Table 8-1). The monitoring and forecasting tools are produced on a monthly basis and includes several drought indicators from two main data sources (GPCC and ECMWF). Both, probabilistic and deterministic seasonal forecasts are displayed taking advantage of the ability of the Standardized Precipitation Index (SPI) in detecting droughts. A drought vulnerability and risk analysis is displayed as well. The information included follows the well-established concept of monitoring, forecasting, warning and response chain and is relevant the set-up of a continental early warning system.

Table 8-1 Characteristics of the products included in the Pan-African Map viewer

<i>Product</i>	<i>resolution</i>	<i>period</i>	<i>Source</i>	<i>Update</i>
<u>MONITORING PRODUCTS</u>				
Total precipitation	1.0°x1.0°	1979-present	GPCC ECMWF Reanalysis	½ month
Precipitation Anomalies: percent of normal (%)	1.0°x1.0°	1979-present	GPCC ECMWF Reanalysis	½ month
Standardized Precipitation Index (SPI)	1.0°x1.0°	1979-present	GPCC ECMWF Reanalysis	½ month
Soil Moisture	1.0°x1.0°	1979-present	ECMWF Reanalysis	½ month
Soil Moisture anomalies: percent of normal (%)	1.0°x1.0°	1979-present	ECMWF Reanalysis	½ month
Vegetation response anomalies (fAPAR)	1 kmx1 km	2002-present	JRC	½ month
Temperature	1.0°x1.0°	1979-present	ECMWF Reanalysis	½ month
Temperature anomalies	1.0°x1.0°	1979-present	ECMWF Reanalysis	½ month
<u>SEASONAL FORECASTS</u>				
SPI probabilistic forecast	1.0°x1.0°		ECMWF S4 system	½ month



SPI ensemble mean forecast	1.0°x1.0°	ECMWF S4 system	½ month
<u>DROUGHT VULNERABILITY AND RISK</u>			
Drought Vulnerability Index	Basin level/Country level	JRC	static
Drought Hazard Index	Basin level	JRC	static
Drought Risk	Basin level/Country level	JRC	static

8.1 MONITORING PRODUCTS

The main monitoring products relies on precipitation and their related indicators as precipitation anomalies (% of normal) and the Standardized Precipitation Index (SPI). GPCP and ERA-Interim precipitation datasets are used as the main sources of precipitation. ERA-Interim monthly temperature and soil moisture including their anomalies are also displayed. The vegetation response is assessed through the anomaly of fAPAR (fraction of Absorbed Photosynthetically Active Radiation): 10-day time composite, 1 km spatial resolution, derived from the SPOT-VEGETATION instrument. The selected indicators and datasets were selected after having been tested at regional and continental scale (see DEWFORA reports D4.2; D4.3; D6.3; Naumann et al., 2012; Dutra et al., 2013a and Naumann et al., 2013a).

During the project the potential of implementing different drought indicators to improve drought monitoring capabilities at continental scale was explored. Several global datasets and drought indicators based on re-analysis, gridded observation, and remote sensing data were tested. At regional level the capabilities of each indicator and dataset on five regions on the African continent (Oum-er-Rbia, Eastern Nile, Niger, Limpopo and the Great Horn of Africa) were compared.

The five precipitation datasets used in this study were the ERA-Interim reanalysis (0.5°x0.5° resolution from 1979 to 2010), the Tropical Rainfall Measuring Mission (TRMM) satellite monthly rainfall product 3B43 (0.25°x0.25° resolution from 1998 to 2010), the Global Precipitation Climatology Centre (GPCP) gridded precipitation dataset V.5 (1°x1° resolution from 1901 to 2010), the Global Precipitation Climatology Project (GPCP) Global Monthly Merged Precipitation Analyses (2.5°x2.5° resolution from 1979 to 2010), and the Climate Prediction Center Merged Analysis of Precipitation (CMAP, 2.5°x2.5° resolution from 1979 to 2010).

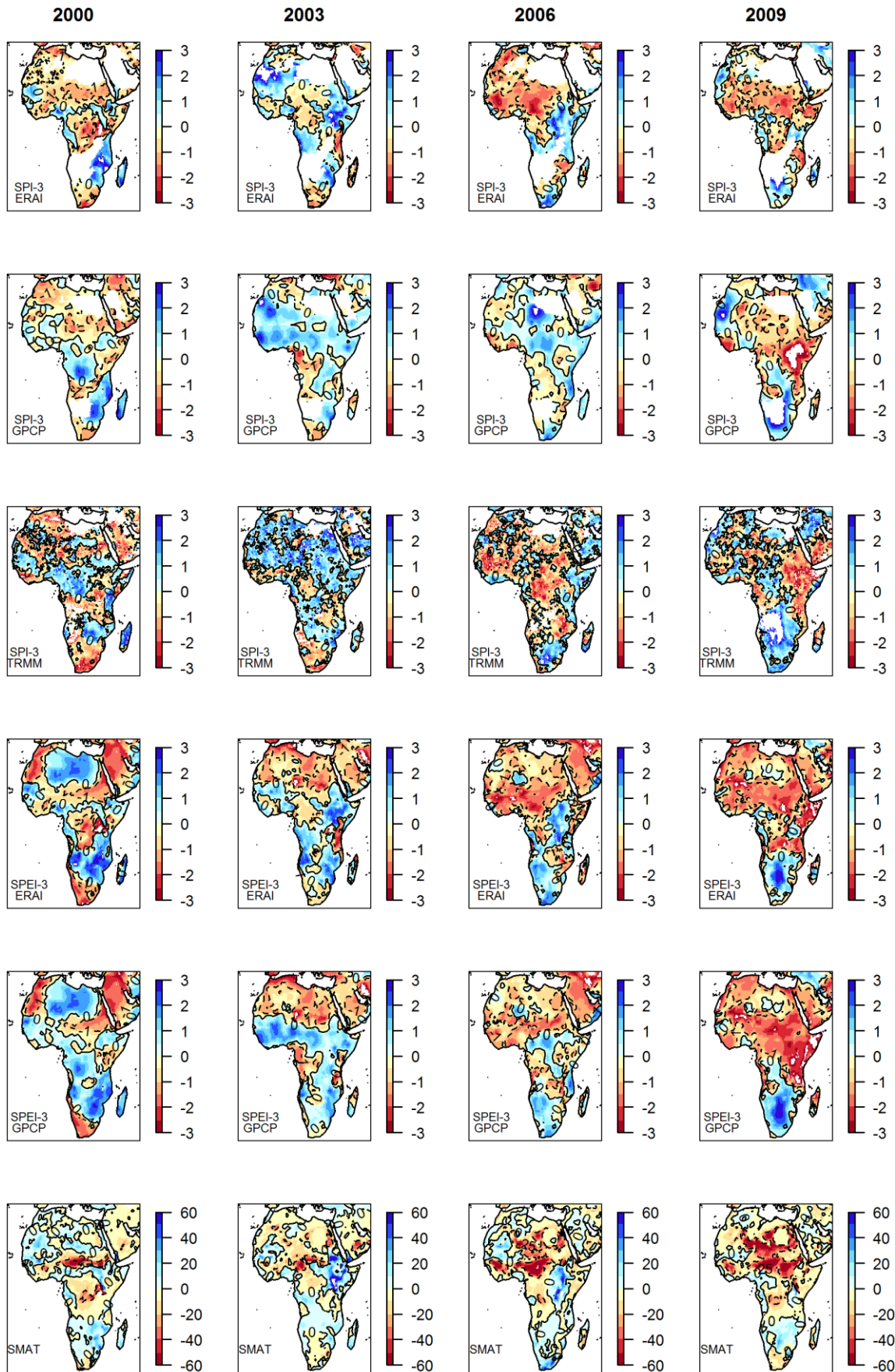


Figure 8-1 Monthly anomalies in SPI-3 (ERAI, GPCP, TRMM), SPEI (ERAI and GPCP) and Soil Moisture Anomalies (SMA) for July 2000, 2003, 2006 and 2009. Solid lines indicates the zero contour.



The set of meteorological and hydrological drought indicators proposed included the Standardized Precipitation index (SPI), the Standardized Precipitation-Evaporation Index (SPEI), the Standardized Run-off index (SRI), the Soil Moisture Anomalies (SMA). Also remote sensing products as the Normalized Difference Water Index NDWI, the fraction of Absorbed Photosynthetically Active Radiation (fAPAR) and the growing season length (GSL) anomalies were tested. The monthly patterns of droughts over Africa depicted by some of the indicators proposed are showed in Figure 8-1.

The main results that come out from the analysis shows that the comparison of the annual cycle and monthly precipitation time series using the different datasets shows a general agreement in the timing of the precipitation peaks, including in the Great Horn of Africa area that has two rainy seasons. The main differences are observed thus in the ability to represent the magnitude of the wet seasons and extremes. Moreover, for the areas that are under drought, all the datasets agree with the time of drought onset and recovery although this agreement varies with the threshold selected to define the drought conditions, and there are sometimes disagreements on the area affected.

The comparative analysis between TRMM, ERAI, GPCP and GPCC datasets suggests that it is feasible to use GPCC or TRMM time series for reliable drought monitoring over Africa. Also ERAI precipitation dataset perform well outside tropical areas.

All the drought indicators analysed at continental level showed a good agreement in North West and Southern Africa, while a low agreement was observed in Central Africa. A good agreement is also observed between SPI (TRMM) and SPI (ERAI) in east Africa. A low agreement of the indicators over Central Africa reflects the high uncertainty present in the precipitation datasets. The comparison between different SPI estimations suggest that the main sources of error are due to the uncertainties in the datasets (lack of ground information, estimation algorithms, parameterization of the convection, etc.) rather than the estimation of the distribution parameters.

The integrated use of two different sources of information in the Horn of Africa, meteorological and remote sensing derived vegetation indices, shows great potential to synergistically monitor drought events.

8.2 SEASONAL FORECASTS

The meteorological seasonal forecast relies in the ECMWF S4 model. This model has a TL255 horizontal resolution (about 0.7° in the grid-point space, same as ERAI) with 91 vertical levels in the atmosphere. The ocean model has 42 vertical levels with a horizontal resolution of approximately 1° . The seasonal forecast generates 51 ensemble members in real-time, with 30 years (1981-2010, 15 ensemble members) of back integrations (hindcasts). The lead time is 7 months, including the month of issue. The two main outputs are the forecasted SPI following a probabilistic or a deterministic approach. In both the cases the SPI is computed with GPCC data as monitoring product merged with the S4 forecasts



(DEWFORA reports D4.2; D6.5; Dutra et al., 2013a and Dutra et al., 2013b). A detailed description of the ECMWF forecast products and implementation is presented in this report. The "PCR-GLOBWB-Africa" is a continental scale version of the distributed global hydrological model PCR-GLOBWB (PCRaster GLOBal Water Balance Model) (van Beek and Bierkens 2009), which was set up for the African continent in an earlier stage of this project. The PCR-GLOBWB was one of the 16 different land surface and hydrological models reviewed earlier in the project deliverable D4.5.

8.3 DROUGHT VULNERABILITY AND RISK

The drought vulnerability and risk were assessed at country and basin level following a socio-economic approach (see DEWFORA D3.1, D6.4 and Naumann et al., 2013b for further details).

The methodology used to compute the Drought Vulnerability Index (DVI) integrates both quantitative and qualitative characterisations of drought vulnerability at different spatial scales.

The term vulnerability is used in the analysis to convey the characteristics of a system or social group that makes it susceptible to suffer the consequences of drought. For example, although the direct impact of precipitation deficiencies may be a reduction of crop yields, the underlying cause of this vulnerability to meteorological drought may be that the farmers did not use drought-resistant seeds - either because they did not believe in their usefulness, their costs were too high, or because of some commitment to cultural beliefs. Another example could be farm foreclosure related to drought; the underlying cause of this vulnerability could be manifold, such as small farm size because of historical land appropriation policies, lack of credit for diversification options, farming on marginal lands, limited knowledge of possible farming options, a lack of local industry for off-farm supplemental income, or government policies.

During the construction process of the composite indicator the sources of uncertainty were tacked into account, while the inference process was as objective and simple as possible. The validation processes of the indicator was divided in three main steps: (i) Definition of the components of drought vulnerability, (ii) selection of variables and their normalisation, and (iii) model validation through a weighting and sensitivity analysis, and comparison with other indicators. A detailed analysis on the weighting scheme adopted as well as a comparison with the impacts of previous drought disasters may help in the stakeholders' acceptance of the indicator.

The drought vulnerability indicator constructed using socio-economic data at country level explores some of the complex processes that could lead to social drought vulnerability. However, it must be used critically taking into account that its construction relies on some subjective level of expert knowledge and theoretical assumptions. According to this analysis,

the countries classified with higher relative vulnerability are Somalia, Mali, Ethiopia, Niger, Burundi and Chad (Figure 8-2).

This kind of analysis can be combined with the advances in seasonal forecast skill (Dutra et al., 2013c) opening the possibility for improved drought early warning systems. However, the implementation of such systems also requires an understanding of the social capacity to use the forecast.

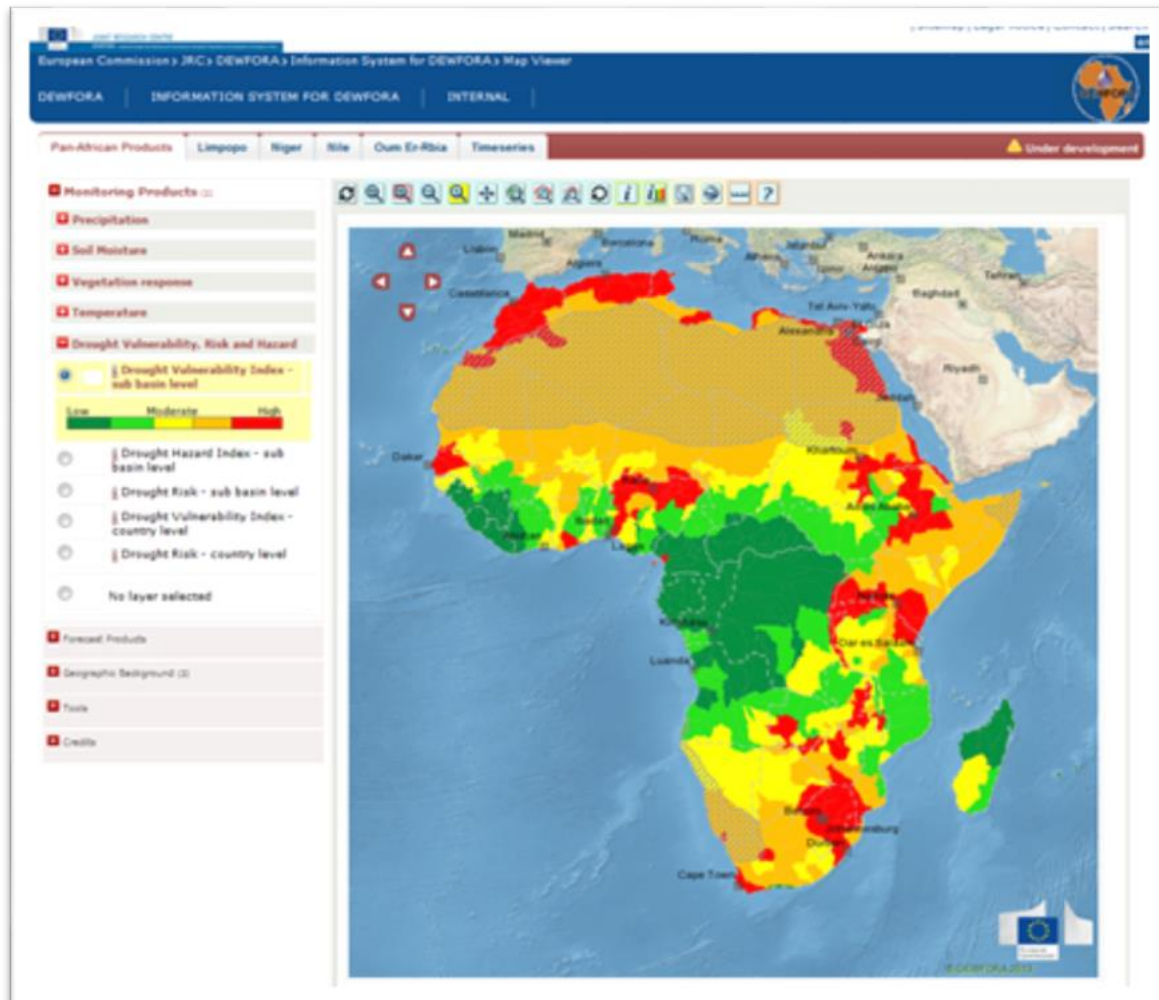


Figure 8-2. Drought Vulnerability Index at sub basin level as displayed in the map viewer with country boundaries and populated places.

8.4 GEOGRAPHICAL BACKGROUND

A number of ancillary data sets are also available such as climate classifications (Aridity Index and Köppen-Geiger Classification, see Spinoni et al., 2013 for further details), land cover and soil maps (Land cover, Agricultural Management Factor, Soil Fertility Index), water resources (Irrigation cropping pattern zones, Surface water bodies and River Basins), and population indicators (population Density and Infant Mortality Rate).

Many of those layers are visualized in DEWFORA as Web Map Services (WMS) from FAO, such as Dominant Soils, Soil Fertility Index, Dynamic Map of Holdridge Life-Zone, Irrigation



cropping patterns, etc. This means that data reside on FAO server, so that they are maintained, updated and stored on their own server.

